ORGANOMETALLICS

Article

pubs.acs.org/Organometallics

Synthesis, Structural Characterization, and Catalytic Evaluation of Phosphinoferrocene Ligands Bearing Extended Urea-Amide Substituents

Hana Solařová, Ivana Císařová, and Petr Štěpnička*

Department of Inorganic Chemistry, Faculty of Science, Charles University in Prague; Hlavova 2030, 128 40 Prague, Czech Republic

Supporting Information

ABSTRACT: New phosphinoferrocene ligands bearing extended polar amidourea pendants with the general formula $Ph_2PfcCONHCH_2CH_2NHCONR_2$ (**1**; $R_2 = H_2$ (**b**), H/Et (**c**), Me_2 (**d**), H/Ph (**e**)) and their model bis-amide $Ph_2PfcCONHCH_2CH_2NHCOCH_3$ (**1a**) were prepared in good yields by amidation of 1′-(diphenylphosphino)-ferrocene-1-carboxylic acid (Hdpf) with the appropriate amines in the presence of peptide coupling reagents. These ferrocene-based phosphinoureas were further employed as ligands in palladium(II) complexes with η^3-allyl and NC-chelating supporting ligands: viz., $[PdCl(\eta^3\text{-}C_3H_5)(\mathbf{1}\text{-}\kappa P)]$ (**5a–e**) and $[PdCl(L^{NC})(\mathbf{1}\text{-}\kappa P)]$ (**6a–e**; L^{NC} = [2-(dimethylamino-κN)methyl]phenyl-κC^1). Both the free ligands and their Pd(II) complexes were characterized by spectroscopic methods (multinuclear NMR, IR, and MS) and by elemental analysis. The molecular structures of **1b**·CH_3OH, **1c**, **5b,c**, **6a**, and two additional model complexes, $[PdCl(\eta^3\text{-}C_3H_5)(Hdpf\text{-}\kappa P)]$ (**5f**) and $[PdCl(\eta^3\text{-}C_3H_5)(Ph_2PfcCONH_2\text{-}\kappa P)]$ (**5g**), were determined by single-crystal X-ray diffraction analysis. All Pd(II) complexes were evaluated as catalysts in the cross-coupling of boronic acids and acyl halides to give ketones in a toluene/water biphasic mixture. Extensive reaction studies with compound **5e**, which not only exerts good catalytic activity but is also readily accessible in a defined crystalline form, demonstrated efficient coupling reactivity for unsaturated substrates such as (substituted) benzeneboronic acids *and* benzoyl chlorides. The results also revealed that reaction difficulties encountered with less reactive substrates (e.g., insoluble aromatic boronic acids and all saturated aliphatic boronic acids) can be avoided by properly selecting the reaction partners, for example through transposition of substituents between reaction partners. Three representative benzophenones (4-fluoro-, 4-nitro-, and 4,4′-dinitrobenzophenone) were structurally characterized by single-crystal X-ray crystallography.

INTRODUCTION

Phosphinoferrocene donors have advanced to the forefront of ligand design, due to their unique structural versatility and many applications in both laboratory- and industrial-scale catalytic processes.[1] The wide practical success of phosphinoferrocene donors has naturally led to the development of several advanced ligand forms, such as those grafted onto dendrimeric[2] or solid supports,[3] as well as water-soluble ligands generated through the introduction of hydrophilic polar substituents.[4]

In previous work, we have focused on phosphinoferrocene carboxamides,[5] a class of versatile and structurally modular ligands that can be conveniently accessed via amidation reactions of various functional building blocks. For instance, amide coupling reactions of 1′-(diphenylphosphino)ferrocene-1-carboxylic acid (Hdpf)[6] with appropriately substituted amines allowed us to prepare donors with increased solubility in polar solvents, including water,[7] as well as phosphinoferrocene ligands that are equipped with a specifically positioned additional donor site and can therefore function as flexible, donor-asymmetric trans-spanning ligands.[8] Other recent studies using (non-ferrocene) phosphinocarboxamide ligands include the preparation of coordination compounds that primarily assemble via hydrogen bonds in the solid state[9] and the synthesis of multinuclear Cu(I) complexes[10] and new ligands for Pd-catalyzed organic transformations.[11]

In the search for new ligand types, we have decided to prepare novel phosphinoferrocene carboxamides bearing urea-containing substituents at the amide nitrogen, anticipating that the urea moieties could possibly endow the resulting phosphine donors with specific properties, such as enhanced hydrogen-bonding ability, increased water solubility, and coordination variability imparted by the additional donor groups. Ligand design through the modification of selected phosphine donors via introduced functional urea moieties is not unprecedented but has only been employed in a limited number of cases. For instance, organic phosphines possessing urea substituents (compounds **A–C** in Chart 1)[12] have been shown to readily associate via hydrogen-bonding interactions of their urea

Received: June 26, 2014
Published: August 1, 2014

   dx.doi.org/10.1021/om5006758 | *Organometallics* 2014, 33, 4131–4147

Chart 1

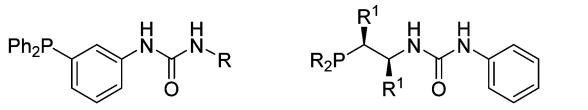

R = Ph (**A**), CH_2CO_2Et (**B**) $R_2P = Ph_2P$, stereogenic phosphine
R^1 = H and Ph (**C**)

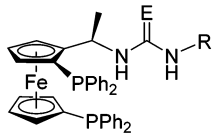

E = O, S; P = aryl, CH(Me)Ph (**D**)

pendants, which in turn affects their coordination and catalytic properties. Another series of ligands combining the chiral scaffold of the archetypal BPPFA ligand[13,1] with (thio)urea tags (see structure **D** in Chart 1; BPPFA = 1,1′- bis-(diphenylphosphino)-2-(1-(dimethylamino)ethyl)ferrocene) was recently prepared and tested in the Rh-catalyzed hydrogenation of nitroalkenes.[14]

In the chemistry of phosphinoferrocene donors, urea has only scarcely been used as a functional modifying group, in contrast with the numerous studies performed with ferrocenyl-substituted ureas as electrochemical sensing devices.[15] In fact, the only examples appear to be the aforementioned BPPFA derivatives (**D** in Chart 1) and several other compounds in which urea moieties were either employed as defined structural linking groups during the preparation of immobilized phosphinoferrocene ligands[3c−f] or introduced via the reactions of phosphinoferrocenecarboxylic acids with carbodiimide reagents.[16] The lack of knowledge regarding phosphinoferrocene-urea ligands led us to design and prepare a series of Hdpf-based amides with substituents bearing a urea moiety at the terminal position (Chart 2).

Chart 2. General Formulation of the Ligands Targeted in This Study

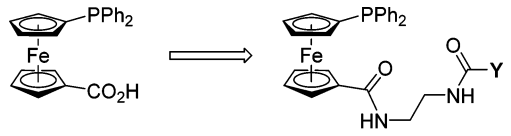

Hdpf **1** (various Y)

In this contribution, we report the preparation of a series of phosphinoferrocene donors **1** that possess ethane-1,2-diyl extended urea-amide tags and their structural characterization. We also describe the results of our investigation into their coordination chemistry with palladium(II) as a model soft metal ion and catalytic properties of the obtained complexes in Pd-catalyzed cross-coupling of boronic acids and acyl halides to give ketones.

RESULTS AND DISCUSSION

Synthesis and Characterization of Ligands. To prepare the targeted ligands, we chose a late-stage assembly approach, having prepared the necessary functional amines before the final amidation with Hdpf. The C_2-extended, urea-substituted building blocks **4a−e** were obtained by reacting free or N-Boc-monoprotected 1,2-diaminoethane (**2a**,**b**, respectively) with the appropriate reagents, followed by subsequent deprotection[17] (Scheme 1). These rather standard reactions generally proceeded well, affording the desired amines as hydrochlorides in good yields. The only problematic reaction proved to be the synthesis of **4b**, bearing a monosubstituted urea moiety. When we followed a procedure from the literature[18] based on the direct carbamoylation of **2a** with in situ generated HNCO, the reaction produced a mixture of the desired product and **2a**·2HCl, which could not be efficiently separated by means of chromatography or fractional crystallization. Fortunately, however, the presence of the side product did not pose any problems during the subsequent amidation reaction or the following workup procedure.

The resulting ω-functionalized amine hydrochlorides (**4a−e**) were in turn reacted with Hdpf in the presence of 1-hydroxybenzotriazole and 1-ethyl-3-[3-(dimethylamino)-propyl]carbodiimide as peptide coupling agents[19] and triethylamine as an HCl scavenger to afford the desired functional amides in good to excellent yields (Scheme 2; yields 52−95%).

The resulting amides were characterized by spectroscopic methods (multinuclear NMR and IR spectroscopy and electrospray ionization (ESI) mass spectrometry), and their formulations were further confirmed by elemental analyses or from high-resolution mass spectra. The NMR spectra of **1a−e** display the resonances due to the 1′-(diphenylphosphino)-ferrocen-1-yl unit at the expected positions, as well as the signals of the $CONH(CH_2)_2NHCO$ spacer and its terminal substituent (Y in Scheme 2). Signals in the $^{31}P\{^1H\}$ NMR spectra are all found at δ_P ca. −18.1 (in DMSO-d_6), similar to the parent acid signal.[20] In the IR spectra of **1b−e**, three strong bands are observed in the range 1635−1550 cm^{-1}, attributable to C═O stretching and N−H bending vibrations. Compound **1a**, which possesses a terminal acetamido substituent rather than a urea unit, expectedly displays only two bands at 1636 and 1552 cm^{-1}.

Compounds **1b**,**c** afforded crystals suitable for X-ray diffraction analysis. The former compound was isolated in the form of the stoichiometric solvate **1b**·CH_3OH upon crystallization from methanol/diethyl ether/hexane, whereas the latter compound crystallized in its unsolvated form from dichloromethane/methanol/hexane. Both compounds crystallized with the symmetry of the common triclinic space group $P\bar{1}$. However, only **1c** resulted with the minimum number of formula units per unit cell ($Z = 2$), while the structure of its *N*-ethyl analogue **1b** contained two structurally independent molecules of the amide and the solvent (i.e., one CH_3OH molecule per molecule of **1b**). The molecular structures of **1b** and **1c** are presented in Figures 1 and 2, respectively, and their selected geometric parameters are summarized in Table 1.

The overall molecular geometries of **1b** and **1c** are quite similar. In fact, the only significant difference in their molecular structures can be detected in the mutual orientation of the substituents at the ferrocene unit. Whereas the cyclopentadienyl rings in molecule 1 of **1b** and in compound **1c** are close to a staggered anticlinal conformation (ideal value τ = 108°), those in **1b**, molecule 2, assume an intermediate conformation between staggered anticlinal and synclinal eclipsed (ideal value τ = 72°; for an overlap of the independent molecules of **1b**, see the Supporting Information, Figure S1). This difference can be attributed to crystal-packing effects. All molecules are comprised of regular ferrocene units with similar Fe−C distances (**1b**, molecule 1, 2.028(3)−2.066(4) Å; **1b**,

dx.doi.org/10.1021/om5006758 | *Organometallics* 2014, 33, 4131−4147

Scheme 1. Preparation of Hydrochlorides of ω-Functionalized Amines

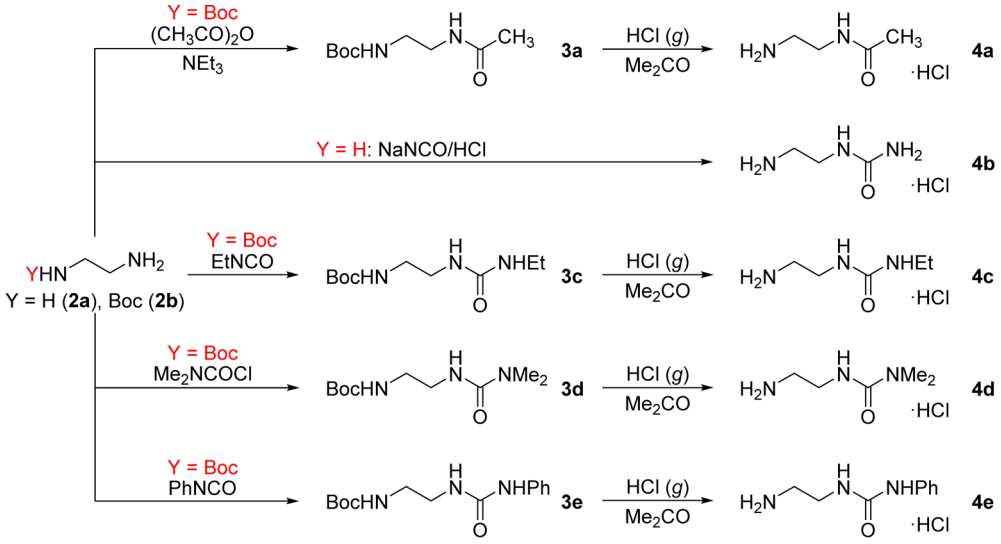

Scheme 2. Preparation of Amides 1a–e[a]

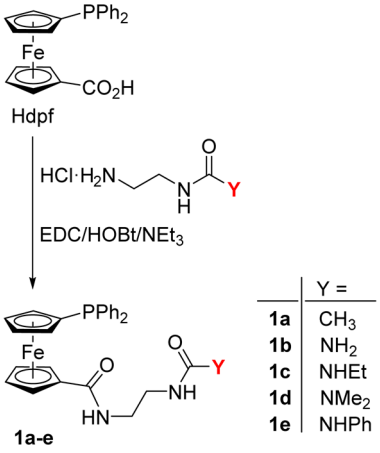

[a]Abbreviations: HOBt, 1-hydroxybenzotriazole; EDC, 1-ethyl-3-[3-(dimethylamino)propyl]carbodiimide.

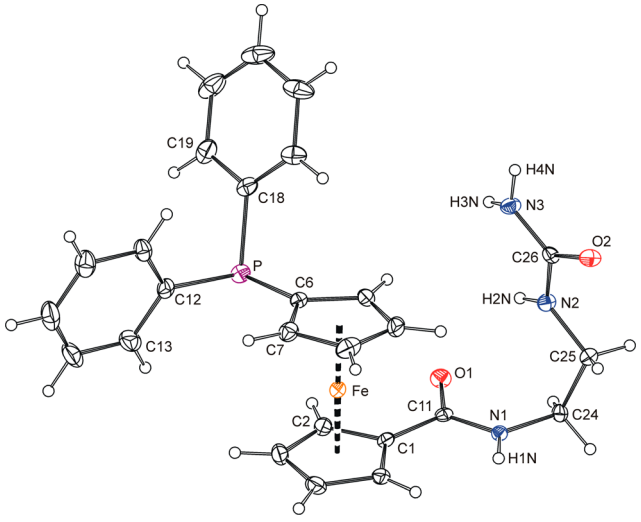

Figure 1. View of molecule 1 in the structure of **1b**·CH_3OH, illustrating the atom-labeling scheme. Non-hydrogen atoms are represented by displacement ellipsoids at the 30% probability level.

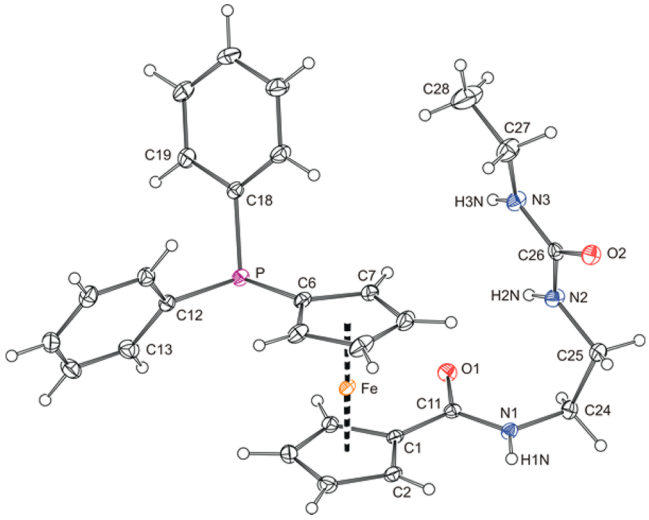

Figure 2. View of the molecular structure of **1c** with displacement ellipsoids scaled to the 30% probability level.

molecule 2, 2.020(4)–2.066(4) Å; **1c**, 2.030(2)–2.067(2) Å) and tilt angles below ca. 5°. The ferrocene-bound amide groups are slightly twisted with respect to the plane of their parent cyclopentadienyl ring (φ angle in Table 1), and the amide pendants are oriented upward (i.e., toward the other cyclopentadienyl) such that the nitrogen substituents at the connecting C24–C25 bonds assume a gauche conformation. Finally, the urea moieties exert the general geometry[21] and render the entire C25–N2–C26(O2)–N3–C27 terminal fragment practically planar.

The crystal packing of **1b**·CH_3OH (Figure 3, Table 2) is based on mutually analogous,[22] striplike arrays, exclusively built up from molecules 1 or 2. These molecules assemble into centrosymmetric dimer units via the typical[23] bifurcated hydrogen bonds between the NHCONH units and the amide oxygen, and the dimers are further interlinked via N–H···O=C interactions. The solvent molecules positioned between these strips connect the formed ribbons into infinite layers located around the (0,1,−1) plane. The phosphinoferrocenyl moieties placed above and below these layers separate the polar, hydrogen-bonded sheets from each other.

dx.doi.org/10.1021/om5006758 | Organometallics 2014, 33, 4131–4147

Table 1. Selected Distances (Å) and Angles (deg) for 1b·CH_3OH and 1c[a]

	1b·CH_3OH		
param	molecule 1 (n = 1)	molecule 2[b]	1c (n = void)[c]
Fe−Cg1	1.652(2)	1.651(2)	1.6519(7)
Fe−Cg2	1.653(2)	1.653(2)	1.6487(7)
∠Cp1,Cp2	4.7(2)	4.6(2)	3.86(9)
τ	102.8(2)	−87.9(3)	105.6(1)
Pn−C6	1.814(3)	1.819(4)	1.813(2)
Pn−C12	1.842(4)	1.834(4)	1.830(1)
Pn−C18	1.837(4)	1.833(4)	1.832(2)
C1−C11	1.482(4)	1.479(4)	1.478(2)
C1−On1	1.238(4)	1.237(4)	1.245(2)
C1−Nn1	1.341(4)	1.342(4)	1.339(2)
On1−C11−Nn1	122.4(3)	122.5(3)	122.5(1)
Nn1−C24	1.453(4)	1.452(4)	1.454(2)
φ	5.8(4)	6.7(4)	7.2(2)
C25−Nn2	1.446(4)	1.446(4)	1.451(2)
C26−Nn2	1.351(5)	1.341(4)	1.354(2)
C26−Nn3	1.345(4)	1.353(4)	1.349(2)
Nn2−C26−Nn3	116.7(3)	116.0(3)	115.6(1)
C26−On2	1.250(4)	1.244(4)	1.242(2)
Nn1−C24−C25−Nn2	−59.3(4)	63.2(4)	−60.5(2)

[a]Cp1 and Cp2 are amide- and Ph_2P-substituted cyclopentadienyl rings, respectively. Cg1 and Cg2 denote their centroids. τ is the torsion angle C6−Cg1−Cg2−C1, and φ is the dihedral angle subtended by the amide moiety (O═C−N) and the Cp1 plane. [b]The atoms in the independent molecules of **1b** are labeled analogously. The labels of the carbon atoms in molecule 2 were obtained after adding 50 to the numerical part of the respective label in molecule 1, and the labels of the other heavy atoms (Fe, P, O, and N) have their first digit changed to 2. The atomic labels given in the far left column belong to molecule 1. [c]Further data: N3−C27 1.448(2), N3−C27−C28 111.5(2).

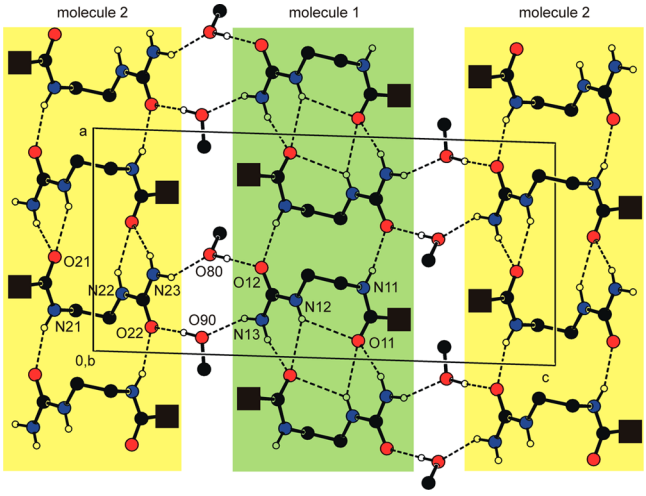

Figure 3. Projection of the hydrogen-bonded layer in the structure of **1b**·CH_3OH onto the crystallographic ac plane. The hydrogen bond parameters are presented in Table 2. For clarity, only NH hydrogens are shown, and the bulky phosphinoferrocenyl units are replaced with black squares. The strips formed from the structurally independent molecules are highlighted with light green (molecule 1) and light yellow (molecule 2) backgrounds.

In contrast, the solid-state assembly of **1c** is relatively simple, reflecting a better match between the number of strong hydrogen bond donors (NH groups) and acceptors (C═O

Table 2. Hydrogen Bond Parameters for 1b·CH_3OH

D−H···A[a]	D···A (Å)	angle at H (deg)
	Molecule 1	
N11−H1N···O12^{i}	2.868(3)	155
N12−H2N···O11^{ii}	3.239(3)	144
N12−H2N···O11[b]	3.181(4)	130
N13−H3N···O11^{ii}	2.869(4)	163
N13−H4N···O90^{ii}	2.853(5)	147
O80−H1O···O12^{i}	2.730(4)	173
	Molecule 2	
N21−H5N···O22^{iii}	2.876(3)	158
N22−H6N···O21^{iv}	3.062(3)	147
N23−H7N···O21^{iv}	2.869(4)	155
N23−H8N···O80^{v}	2.835(4)	141
O90−H2O···O22^{iv}	2.732(4)	176

[a]D = donor, A = acceptor. Symmetry codes: (i) 1 − x, 1 − y, 1 − z; (ii) 2 − x, 1 − y, 1 − z; (iii) 2 − x, 2 − y, −z; (iv) 1 − x, 2 − y, −z; (v) 1 − x, 1 − y, −z. [b]Intramolecular hydrogen bond.

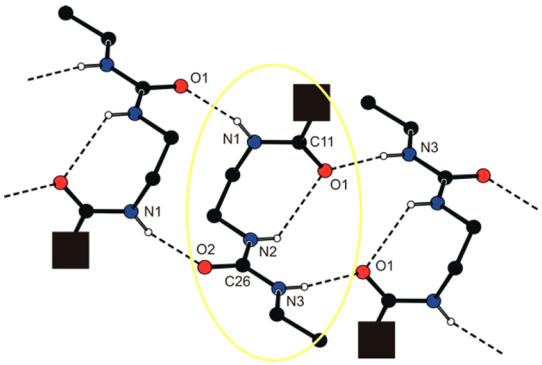

Figure 4. Section of the infinite, hydrogen-bonded ribbons in the structure of **1c**. For clarity, only the NH hydrogens are depicted, and the bulky phosphinoferrocenyl units are replaced with filled black squares. The hydrogen bond parameters are as follows: N1−H1N···O2^{i}, N1···O2 = 2.847(2) Å, angle at H1N 159°; N2−H2N···O1, N2···O1 = 3.113(2) Å, angle at H2N 130°; N3−H3N···O1^{ii}, N3···O1 = 2.860(2), angle at H3N 171°; C15−H15···O2^{iii} (not shown in the figure), C15···O2 = 3.311(2) Å, angle at H15 143°. Symmetry codes: (i) 1 − x, 1 − y, 2 − z; (ii) 2 − x, 1 − y, 2 − z; (iii) 1 + x, y, z − 1.

moieties; Figure 4). The individual molecules of **1c** associate via N1−H1N···O2/N3−H3N···O1 hydrogen bond pairs. Through the involvement of molecules related by crystallographic inversion, these interactions result in the formation of infinite ribbons oriented parallel to the a axis that are further cross-linked into a three-dimensional array by relatively weaker C−H···O interactions. The N2−H2N moiety, which does not participate in intermolecular hydrogen bonding, forms an intramolecular hydrogen bridge toward O1, albeit with a rather acute angle at the hydrogen atom (130°).

Synthesis of Palladium(II) Complexes. Two series of monophosphine Pd(II) complexes, differing in the auxiliary ligands, were prepared with the aim of evaluating the coordination and catalytic properties of ligands **1** (Scheme 3). Complexes [PdCl(η^3-C_3H_5)(L-κP)] (**5a−e**) were obtained in good yields (from ca. 60% to practically quantitative depending on the isolation procedure) through cleavage of the [PdCl(η^3-C_3H_5)]$_2$ dimer with a stoichiometric amount of the respective ligand **1**. Employing more simple phosphine donors, two additional complexes, [PdCl(η^3-C_3H_5)(Hdpf-κP)] (**5f**) and [PdCl(η^3-C_3H_5)(Ph_2PfcCONH$_2$-κP)] (**5g**; fc =

dx.doi.org/10.1021/om5006758 | Organometallics 2014, 33, 4131−4147

Scheme 3. Synthesis of Palladium(II) Complexes 5 and 6

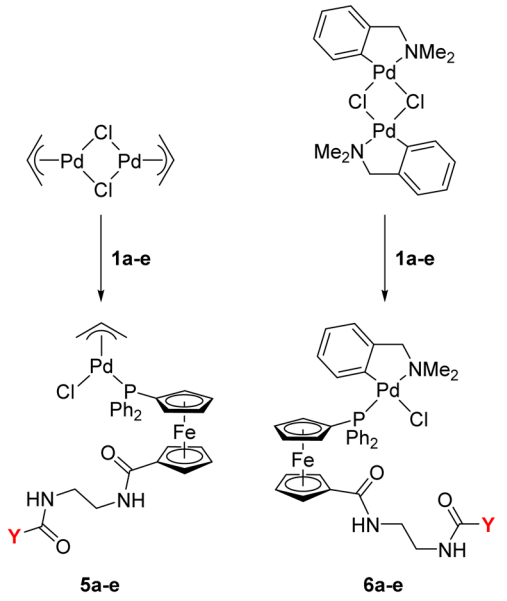

ferrocene-1,1′-diyl), were similarly prepared from Hdpf and its amide.

Complexes with amide ligands, **5a−e** and **5g**, display singlets in their $^{31}P\{^{1}H\}$ NMR spectra at approximately δ_P 12 (in $CDCl_3$) or δ_P 17 (in DMSO-d_6), shifted to lower fields with respect to the signals for their free ligands. The signal of **5f** is observed at δ_P 15.3 (in $CDCl_3$). The ^{1}H NMR spectra of **5a−g** combine signals due to the ferrocene ligand with the characteristic resonances of the five protons located at the η^3-coordinated allyl moiety.[24] The observed broadening of the signals due to the allyl ligand suggests some structural dynamics, as is typical for these types of complexes.[25] The positions of the IR bands that are attributed to the amide and urea moieties observed for complexes **5a−g** generally differ slightly from those of the corresponding free ligand. However, these differences can be accounted for by solid-state effects (hydrogen bonding). The ESI mass spectra of the (η^3-C_3H_5)Pd complexes **5a−g** corroborate their formulations by displaying signals due to $[M - Cl]^+$ as the major ionic species. Both elemental analyses and the NMR spectra indicate that complexes **5a−g** have a tendency to hold residual chlorinated solvents.

The second series of Pd(II) complexes $[PdCl(L^{NC})(L\text{-}\kappa P)]$ (**6a−e**), possessing the 2-[(dimethylamino-κN)methyl]phenyl-κC^1 supporting ligand (L^{NC}), was prepared in a manner analogous to that for the first series (Scheme 3), starting with $[PdCl(L^{NC})]_2$ and ligands **1a−e** (yields >95%). The ^{1}H NMR spectra of **6a−e** support the formulation by revealing signals characteristic for donors **1** and the auxiliary ligand L^{NC}. The ^{31}P NMR resonances of **6a−e** are all located near δ_P 33.0 (in $CDCl_3$), close to that of $[PdCl(L^{NC})(Ph_2PfcCO_2Me\text{-}\kappa P)]$.[26] Similar to the case for **5**, complexes **6a−e** display intense peaks due to $[M - Cl]^+$ in their ESI mass spectra and tend to retain reaction solvents in their bulk structures.

The formulation of Pd(II) complexes was unequivocally corroborated by the single crystal diffraction analyses of **5b,c** and **6a**. The structures of complexes **5f** and **5g**, which contain the model phosphinoferrocene ligands, are presented in the Supporting Information. Compounds **5b** and **5c** (Figure 5 and Table 3) crystallize with their η^3-allyl moieties disordered over two positions that were approximately related by rotation along the axis passing through the Pd atom and the center of the allyl ligand.[27] Nonetheless, this feature corresponds with the known fluxionality of the η^3-allyl complexes[25] and the fact that the allyl units in these particular compounds occupy a space demarcated by the bulkier phosphinoferrocene ligand, whose hydrogen-bonding interactions and van der Waals envelope govern the crystal assembly. In addition, the terminal ethyl group in **5c** is disordered over two positions in the voids defined by the nonpolar (hydrophobic) regions of the complex molecule.

Coordination geometries around the Pd(II) centers in **5b,c** are similar to those determined for $[PdCl(\eta^3\text{-}2\text{-}MeC_3H_4)(L\text{-}\kappa P)]$, where L = Hdpf[28] and $Ph_2PfcCONHCH_2CO_2Me$,[29]

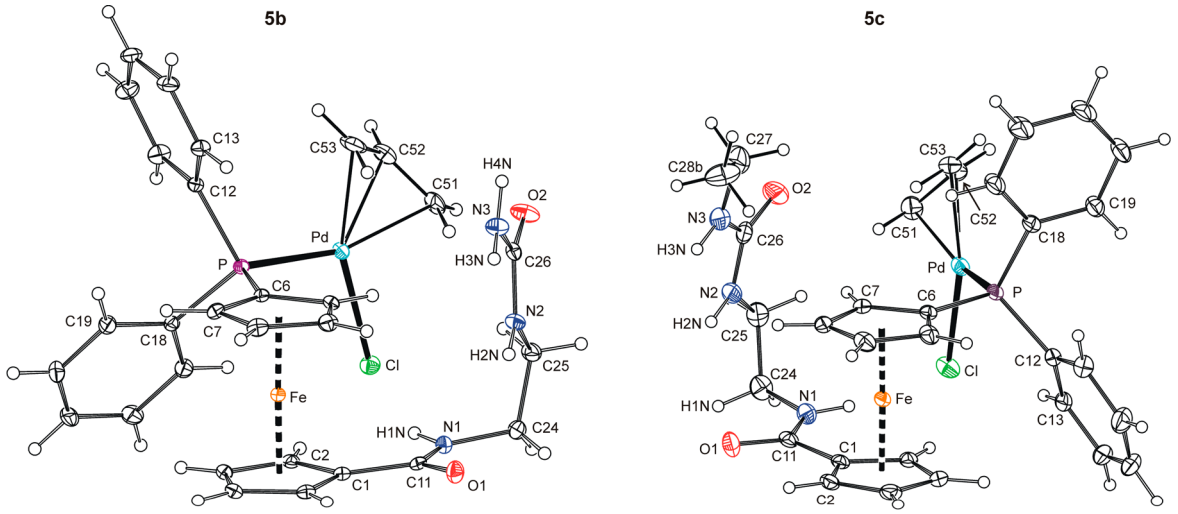

Figure 5. PLATON plots of the molecular structures of **5b** (left) and **5c** (right) at the 30% probability level. For clarity, only the more populated orientations of the disordered moieties are displayed. Coordination geometry parameters for **5b** [**5c**] (in Å and deg): Pd−Cl 2.3887(6) [2.3924(6)], Pd−P 2.3183(6) [2.3167(6)], Cl−Pd−P 104.73(2) [105.59(2)], Pd−C51 2.210(5) [2.303(5)], Pd−C52 2.155(3) [2.216(5)], Pd−C53 2.12(1) [2.138(7)] (data are for the dominating allyl group orientation).

dx.doi.org/10.1021/om5006758 | *Organometallics* 2014, 33, 4131−4147

Table 3. Geometric Parameters (in Å and deg) of the Phosphinoferrocene Ligands in Complexes 5b,c and 6a[a]

param	5b	5c	6a
Fe−Cg1	1.653(1)	1.643(1)	1.646(1)
Fe−Cg2	1.648(1)	1.642(1)	1.646(1)
∠Cp1,Cp2	2.5(1)	1.7(1)	0.8(2)
τ	98.8(2)	−97.9(2)	−143.8(2)
P−C6	1.805(2)	1.803(2)	1.809(3)
P−C12	1.822(2)	1.824(2)	1.816(3)
P−C18	1.825(2)	1.826(2)	1.821(2)
C11−O1	1.233(3)	1.245(3)	1.232(3)
C11−N1	1.340(3)	1.335(3)	1.342(3)
O1−C11−N1	122.5(2)	121.8(2)	122.3(2)
φ	4.4(3)	7.6(2)	6.5(3)
N2−C26−X	115.8(2)[b]	115.7(2)[b]	115.9(2)[c]
C26−O2	1.231(3)	1.237(3)	1.232(3)
N1−C24−C25−N2	63.1(3)	−64.8(3)	171.9(2)

[a]Cp1 and Cp2 are amide- and Ph_2P-substituted cyclopentadienyl rings, respectively. Cg1 and Cg2 represent their centroids. τ is the torsion angle C6−Cg1−Cg2−C1, and φ is the dihedral angle subtended by the amide moiety (O=C−N) and the Cp1 plane. [b]X = N3. [c]X = C27.

respectively. Similar to the case for these reference compounds, the allyl planes in **5b,c** are tilted with respect to the plane defined by Pd and the directly bonded donor atoms Cl and P, with C52 in the meso position diverting from the Pd center. Due to the trans influence of the ligands ($P > Cl^-$),[30] the Pd−C bond lengths decrease gradually from C51 to C53. The geometry of the coordinated phosphinoferrocene ligand in **5b** is similar to that in free **1b** (vide supra). The ferrocene cyclopentadienyls are tilted by 2.5(1)° and bind symmetrically to the Fe atom. Furthermore, the mutual orientation of the ferrocene cyclopentadienyls resembles that of the free ligand. The amide moiety in **5b** is nearly parallel with its bonding cyclopentadienyl ring (Cp1; cf. φ in Table 3), and its substituent extends toward the side of the ferrocene unit and retains a gauche conformation at the C24−C25 bond. A similar orientation can be found in the pair constituted by **1c** and its complex **5c**, wherein the coordination appears to only marginally affect the ligand geometry, including the molecular conformation.

In the solid state, complex **5b** forms bent ribbons that are built up from repeating dimeric units connected via N3−H3N···O1 hydrogen bonds into 18-membered cycles and further stabilized by intramolecular N2−H2N···O1 interactions (though with an acute angle at the H2N atom; Figure 6). These units propagate by translation along the crystallographic *a* axis via bent N3−H4N···Cl interactions. The Pd-bound chloride ligand further acts as an acceptor in the intramolecular N1−H1N···Cl bond.

The crystal assembly of **5c** is relatively simple (Figure 7), based on centrosymmetric dimers that are connected via N3−H3N···O1 interactions. The N1−H1 groups form additional hydrogen bonds with the chloride ligand (intramolecular interactions), while the hydrogen-bonding abilities of the C26=O2 and N2−H2 moieties, buried within the polar domains, remain unexploited.

Compound **6a** (Figure 8 and Table 3) was crystallized in the form of a solvate with diethyl ether and methanol (**6a**·$^1/_2Et_2O$·$^1/_2CH_3OH$). Unfortunately, the solvent molecules were heavily disordered and were thus removed from the

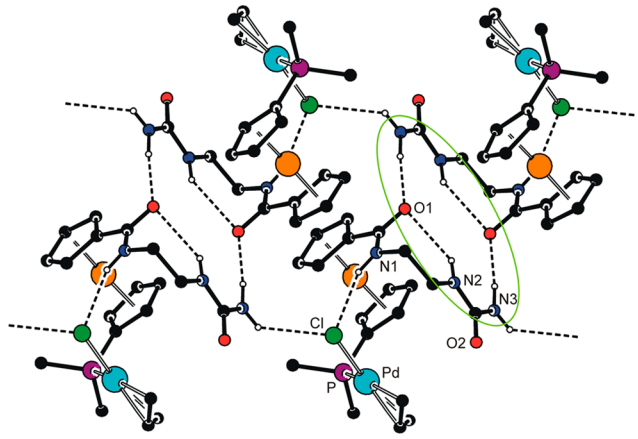

Figure 6. Hydrogen bonds in the crystal structure of **5b**. Only the pivotal carbons from the phenyl rings and hydrogen atoms involved in hydrogen-bonding interactions are shown for clarity. The hydrogen bond parameters are as follows: N1−H1N···Cl, N1···Cl = 3.317(2) Å, angle at H1N 157°; N2−H2N···O1, N2···O1 = 3.273(3) Å, angle at H2N 145°; N3−H3N···O1^{i}, N3···O1 = 2.893(3) Å, angle at H3N 169°; N3−H4N···Cl^{ii}, N3···Cl = 3.388(2) Å, angle at H4N 136°. Symmetry codes: (i) $1-x, 1-y, 2-z$; (ii) $1+x, y, z$.

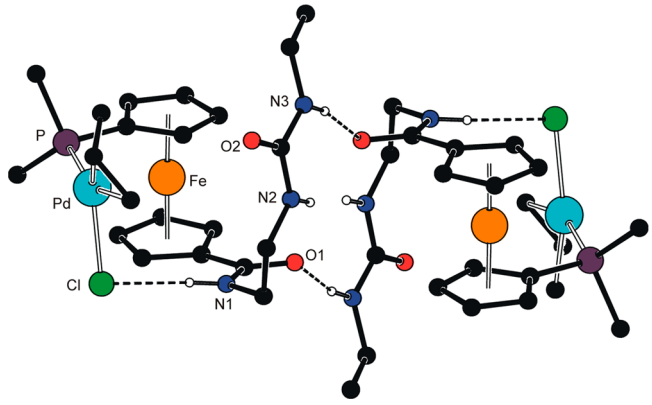

Figure 7. Hydrogen bonds in the crystal structure of **5c**. For clarity, only the P-bound carbon atoms from the phenyl rings and hydrogens involved in hydrogen-bonding interactions are shown. The hydrogen bond parameters are as follows: N1−H1N···Cl, N1···Cl = 3.296(2) Å, angle at H1N 163°; N3−H3N···O1^{i}, N3 ···O1 = 2.849(3) Å, angle at H2N 168°. Symmetry code: (i) $-x, 1-y, 1-z$.

structure model using PLATON/SQUEEZE (see the Experimental Section). This structure corroborated the *trans*-P−N arrangements inferred from the NMR data (mainly the $^4J_{PH}$ and $^3J_{PC}$ coupling constants).[31] When the coordination around the Pd atom in **6a** is considered, the structure is comparable to those of $[(\mu\text{-dppf})\{PdCl(L^{NC})\}_2]$[32] and the related monopalladium complexes $[PdCl(L^{NC})(Ph_2PfcY\text{-}\kappa P)]$, where Y = CO_2Me,[26] $CONH_2$,[33] and $CONHCH_2CO_2Me$.[34] The Pd−donor bond lengths increase in the following order: Pd−Cl > Pd−P > Pd−N > Pd−C (span ca. 0.4 Å). This variation in the coordination bond lengths, together with the angular strain imposed by the small metallacycle, result in twisting of the coordination sphere such that the half-planes defined by the {Pd,Cl,P} and {Pd,N3,C40} atoms are mutually rotated by as much as 15.1(1)°. Closure of the interligand angle associated with the metallacycle (N3−Pd−C40 = 81.66(8)°) appears to be compensated via opening of the opposite and adjacent angles (Cl−Pd−P = 92.23(3)°, P−Pd−C40 = 97.49(7)°). The

dx.doi.org/10.1021/om5006758 | *Organometallics* 2014, 33, 4131−4147

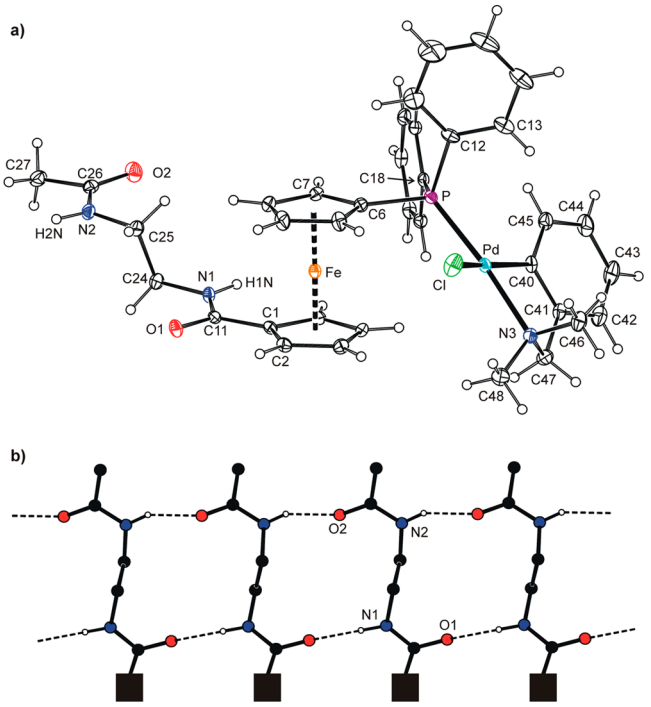

Figure 8. (a) PLATON plot of the molecular structure of **6a** (30% probability). Coordination geometry parameters (in Å and deg): Pd–Cl 2.3910(7), Pd–P 2.2522(7), Pd–N3 2.142(2), Pd–C40 2.009(3), Cl–Pd–P 92.23(3), Cl–Pd–N3 90.10(6), P–Pd–C40 97.49(7), N3–Pd–C40 81.66(8). (b) Simplified diagram of the hydrogen-bonding interactions of **6a**. For simplicity, the bulky phosphinoferrocenyl units with coordinated (L^{NC})PdCl moieties are replaced by black squares, and only NH hydrogens are shown. The hydrogen bond parameters are as follows: N1–H1N···O1^{i}, N1···O1 = 2.951(3) Å, angle at H1N 146°; N2–H2N···O2^{ii}, N2···O2 = 2.789(3) Å, angle at H2N 154°. Symmetry codes: (i) x, $^{1}/_{2} - y$, $-^{1}/_{2} + z$; (ii) x, $^{1}/_{2} - y$, $^{1}/_{2} + z$.

metallacycle itself adopts a twisted-envelope conformation, with the N3 atom at the tip position.[35]

The ferrocene unit in **6a** is tilted by less than 1°, and the attached amide unit is rotated by 6.5(3)°. However, the overall conformation of the phosphinoferrocene ligand in **6a** differs from that observed in the structures of all other structurally characterized compounds mentioned in this study. The substituents at the ferrocene moiety in **6a** are mutually more distant, assuming a practically ideal anticlinal eclipsed conformation. Furthermore, the substituents at the C24–C25 bond are close to anti (see parameters in Table 3), which directs the amide pendant to the side, away from the ferrocene unit.

The individual molecules in the crystal of **6a** associate through N–H···O=C hydrogen bonds into one-dimensional ladderlike assemblies, propagating in the direction of the c axis. These ribbons are decorated with bulky fcPPh$_2$PdCl(L^{NC}) groups, arranged in an up–down manner at one side of the chain due to the crystallographic symmetry (glide plane; Figure 8b).

Catalytic Evaluation. The catalytic potential of donors **1a–e** was evaluated in the palladium-mediated cross-coupling of boronic acids with acyl halides to afford ketones. This particular reaction,[36] formally equivalent to carbonylative Suzuki–Miyaura cross-coupling,[37] has attracted considerable attention since its discovery in 1997,[38,39] as it offers a facile, selective, and functional group tolerant alternative to the conventional methods of ketone synthesis, such as oxidative transformations and Friedel–Crafts reaction.[40] Several ligand-free and ligand-supported homogeneous palladium catalysts that efficiently mediate the reaction of unsaturated (mostly aromatic) substrates have been developed.[41] Notably, an initial report has already demonstrated the possibility of performing this cross-coupling reaction in aqueous media. However, only few studies have expanded upon this idea.[42] Considering the structure of the phosphinoferrocene donors reported in this paper, namely the combination of a bulky, soft-donor phosphinoferrocene moiety with a hydrophilic urea tag, we tested their potential catalytic application in an aqueous biphasic reaction system.

The initial screening experiments, aiming to determine the best reaction conditions, were conducted by the coupling reaction of benzoyl chloride (**7a**) and 4-fluorophenylboronic acid (**8i**) to give 4-fluorobenzophenone (**9i**; Scheme 4). Fluorinated boronic acid was used because it allows for easy reaction monitoring by ^{19}F NMR spectroscopy.

Scheme 4. Model Coupling Reaction Used for the Screening Experiments

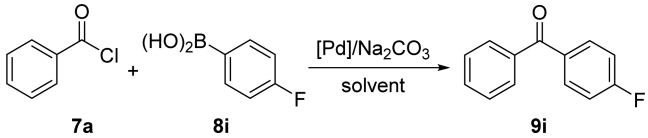

7a **8i** **9i**

Fortuitously, the first reactions tested (for summary, see the Supporting Information, Table S2) with complex **5e** were promising. The reaction of **8i** (1.25 mmol) with **7a** (1.5 mmol or 1.2 equiv) in the presence of 1 mol % of Pd catalyst and sodium carbonate (1.25 mmol) as the base at 50 °C afforded benzophenone **9i** in a 97% NMR yield after 3 h. Decreasing the amount of catalyst to 0.2% did not reduce the yield of the coupling product, and even with 0.1 mol % of the catalyst, the reaction produced **9i** in a 91% NMR yield within 3 h. The reaction also proceeded well with shorter reaction times (1 h) and was not affected much by increasing the amount of either the base or **7a**. Furthermore, the NMR yields achieved at room temperature with 0.2 and 1.0 mol % of Pd did not differ from those obtained at 50 °C (N.B.: the vast majority of the subsequent catalytic reactions were performed at 50 °C with 0.2 mol % of Pd to avoid any influence of temperature fluctuations and to achieve good yields with the less reactive substrates).

The following experiments demonstrated that the catalyst efficacy depends on the structure of the Pd(II) (pre)catalyst. Inspection of the results obtained with the Pd(II) complexes presented in this study and their phosphine-free precursors (Table 4) reveals that η^3-allyl complexes **5a–e** give rise to active catalysts that produce the coupling product in 94–97% NMR yields with 0.2 mol % of Pd loading and short reaction times (50 °C for 1 h). In contrast, the reaction in the presence of 1 mol % (*sic*!) of the precursor [PdCl(η^2-C$_3$H$_5$)]$_2$ afforded **9i** in only 26% NMR yield.[19] In this case, ^{19}F NMR analysis showed an additional signal due to an unknown side product (ca. 23%), as well as resonances attributable to unreacted boronic acid and corresponding boroxine (the rest).[43] The promising results achieved with **5a–e** led us to further simplify the catalyst structure by minimizing the size of the polar group attached to the phosphinoferrocene scaffold. However, the

dx.doi.org/10.1021/om5006758 | Organometallics 2014, 33, 4131–4147

Table 4. Summary of the Catalytic Results Obtained with Pd(II) Complexes 5 and 6[a]

Y in the ligand	complex	NMR yield of **9i** (%)	complex	NMR yield of **9i** (%)
CH_3	**5a**	95	**6a**	91
NH_2	**5b**	95	**6b**	95
NHEt	**5c**	94	**6c**	89
NMe_2	**5d**	97	**6d**	91
NHPh	**5e**	95	**6e**	91
	$[PdCl(C_3H_5)]_2$	26[b]	$[(L^{NC})PdCl]_2$	33[b]

[a]Conditions: 4-fluorophenylboronic acid (1.25 mmol), benzoyl chloride (1.5 mmol), sodium carbonate (1.25 mol), and catalyst (0.2 mol % Pd) in C_6D_6/water (3 mL each) at 50 °C for 1 h. [b]Reaction in the presence of 1 mol % of Pd.

catalytic results were rather disappointing. For instance, $[PdCl(\eta^3\text{-}C_3H_5)(Ph_2PfcCONH_2\text{-}\kappa P)]$ (**5g**) afforded the coupling product **9i** in a relatively lower but still acceptable yield of 87%. In contrast, the reaction in the presence of $[PdCl(\eta^3\text{-}C_3H_5)(Ph_2PfcCO_2H\text{-}\kappa P)]$ (**5f**), containing a free carboxyl group that was expected to increase the solubility of the catalyst in the reaction system through deprotonation of the free carboxyl group by the added base, gave **9i** in only a 7% NMR yield, while the majority of the boronic acid remained unconsumed.

Complexes **6a**–**e**, which employed the L^{NC} supporting ligand, produced yields similar to or slightly lower than their (η^3-allyl)Pd analogues under identical conditions (0.2 mol % of Pd; see Table 4). Even in their case, the precursor complex $[(L^{NC})PdCl]_2$ (1 mol % Pd) resulted in markedly lower yields (33% of **9i**, 67% of unreacted **8i**) than the corresponding phosphine complexes. In view of the collected results, compound **5e** was employed as the catalyst in all subsequent reactions with various substrates because this complex not only exhibited good catalytic activity but was also easily accessible in a defined crystalline form.

As a next step, we investigated the scope of the cross-coupling reaction by varying the reaction components (Scheme 5 and Table 5). Reactions performed with **7a** and differently

Scheme 5. General Scheme for the Cross-Coupling of Acyl Chlorides with Boronic Acids

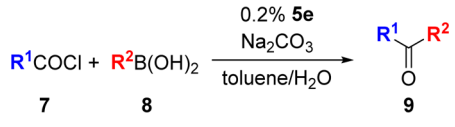

substituted benzeneboronic acids (entries 1–16) proceeded well with substrates bearing methyl, fluoro, chloro, methoxy and trifluoromethyl substituents in the para position. Notably, coupling with the bulky mesitylboronic acid also proceeded reasonably well, providing the coupling product in a 55% isolated yield (entry 6). The yields of ketones achieved in the reactions with 1-naphthylboronic (**8b**) and 4-bromophenylboronic acids (**8k**) were slightly lower (ca. 70%). In the case of the former, the somewhat lower yield reflects the formation of naphthalene (5% isolated yield) as a dehalogenation product, presumably resulting from protonolysis of the oxidative addition product. This side reaction, usually negligible in Suzuki–Miyaura biaryl synthesis,[44] can be facilitated by the bulkiness of the naphthyl group and the availability of protons

Table 5. Assessment of the Substrate Scope and the Role of the Substituents[a]

entry	acyl chloride (R)	boronic acid (R)	product	isolated yield (%)[b]
1	**7a** (Ph)	**8a** (Ph)	**9a**	91
2	**7a**	**8b** (1-naphthyl)	**9b**	71[c]
3	**7a**	**8c** (2-C_6H_4Me)	**9c**	94
4	**7a**	**8d** (3-C_6H_4Me)	**9d**	91
5	**7a**	**8e** (4-C_6H_4Me)	**9e**	91
6	**7a**	**8f** (2,4,6-$C_6H_3Me_3$)	**9f**	55
7	**7a**	**8g** (4-C_6H_4OMe)	**9g**	86
8	**7a**	**8h** (4-C_6H_4COMe)	**9h**	59
9	**7a**	**8i** (4-C_6H_4F)	**9i**	84
10	**7a**	**8j** (4-C_6H_4Cl)	**9j**	91
11	**7a**	**8k** (4-C_6H_4Br)	**9k**	71[d]
12	**7a**	**8l** (4-$C_6H_4CF_3$)	**9l**	87
13	**7a**	**8m** (4-$C_6H_4NO_2$)	**9m**	19
14	**7a**	**8n** (4-C_6H_4CN)	**9n**	42
15	**7a**	**8o** (CH=CHPh)	**9o**	79
16	**7a**	**8p** (CH_2CH_2Ph)	**9p**	0
17	**7c** (2-C_6H_4Me)	**8a**	**9c**	52
18	**7d** (3-C_6H_4Me)	**8a**	**9d**	85
19	**7e** (4-C_6H_4Me)	**8a**	**9e**	85
21	**7g** (4-C_6H_4OMe)	**8a**	**9g**	25
22	**7j** (4-C_6H_4Cl)	**8a**	**9j**	99
23	**7l** (4-$C_6H_4CF_3$)	**8a**	**9l**	99
24	**7m** (4-$C_6H_4NO_2$)	**8a**	**9m**	94
25	**7o** (CH=CHPh)	**8a**	**9o**	52
26	**7p** (CH_2CH_2Ph)	**8a**	**9p**	54
27	**7q** (CH_2Ph)	**8a**	**9q**	40
28	**7g**	**8g**	**9gg**	26
29	**7m**	**8m**	**9mm**	17
30	**7g**	**8m**	**9gm**	2
31	**7m**	**8g**	**9gm**	74

[a]Conditions: catalyst **5e** (0.2 mol %), boronic acid (1.25 mmol), acyl chloride (1.5 mmol), and Na_2CO_3 (1.25 mmol) in toluene/water at 50 °C for 1 h. [b]Average of two independent runs. [c]Naphthalene was isolated as a side product (ca. 5%). [d]4-Benzoyl-4′-bromobiphenyl was also isolated (ca. 10%).

in the present aqueous reaction system. On the other hand, the yield of **9k** was reduced due to the tendency of **8k** to enter competitive Suzuki–Miyaura biaryl coupling as a haloarene, giving rise to 4-benzoyl-4′-bromobiphenyl, which was isolated in approximately 12% yield. Relatively lower yields of the respective ketones were also obtained in the benzoylation of 4-acetylboronic acid (**8h**, 59%), 4-cyanoboronic acid (**8n**, 42%), and, mainly, 4-nitrophenylboronic acid (**8m**, 19%). In the case of **8m** and **8n**, however, the lower yields apparently resulted from low solubility of the boronic acids in the reaction system (toluene), which limited the accessible amount of one of the reactants. Notably, the reaction proceeded well with cinnamylboronic acid, giving *trans*-chalcone in a good isolated yield of 79%, whereas the coupling with 3-phenylpropylboronic acid provided none of the desired ketone. The feasibility of performing "synthetic reactions" on a larger scale was demonstrated for the coupling of **7a** with **8j** at a 10 mmol scale, affording analytically pure ketone **9j** in a virtually quantitative yield.[45]

Additional acylation reactions were performed in an inverted manner: i.e., with substituted acyl chlorides and benzenebor-

dx.doi.org/10.1021/om5006758 | Organometallics 2014, 33, 4131–4147

onic acid (entries 17−27). The reactions of **8a** with 3- and 4-toluoyl chloride, 4-chlorobenzoyl chloride, and 4-(trifluoromethyl)benzoyl chloride afforded the corresponding monosubstituted benzophenones in yields similar to those obtained in the reactions of the respective substituted boronic acids with unsubstituted benzoyl chloride **7a**. The amount of 2-methylbenzophenone obtained from 2-toluic chloride and **8a** was lower, which can be tentatively attributed to steric hindrance. The presence of substituent in the ortho position probably makes the primary oxidative addition of the acyl chloride more difficult, thereby affecting the entire reaction.[37a,46] Even more significant differences were observed in the reactions leading to 4-methoxybenzophenone and *trans*-chalcone. In these reactions, formal transfer of the substituent to the other reaction partner resulted in a pronounced decrease in the reaction yield (**9g**, 25 vs 86%, **9o**, 52 vs 79%). In contrast, the opposite trend was observed with the coupling reactions leading to 4-nitrobenzophenone (**9m**, 94 vs 19%), in which case the coupling reaction was no longer hindered by the low reagent solubility. More importantly, the inverted approach allowed for efficient benzoylation of the less reactive alkylboronic acids (entries 26 and 27). Thus, the coupling between **8a** and 3-phenylpropanoyl chloride afforded 1,3-diphenylpropan-1-one in 54% yield, and a similar reaction with phenylacetyl chloride provided 1,2-diphenylethanone in 40% isolated yield.

The differences observed upon moving the substituent at the benzene ring from one reaction component to the other in the reactions producing monosubstituted benzophenones prompted us to perform more test reactions with the "difficult" substrates possessing 4-methoxy and 4-nitro substituents. The results (entries 28−31 in Table 5) corroborated previous observations in that the reactions of equally substituted substrates (i.e., 4-methoxybenzoyl chloride (**7g**) with 4-methoxybenzeneboronic acid (**8g**) and 4-nitrobenzoyl chloride (**7m**) with 4-nitrobenzeneboronic acid (**8m**)) provided the respective coupling products in relatively modest yields. In the cross-reactions, the coupling of poorly soluble **8m** with **7g** afforded **9gm** in a practically negligible yield (<5%), while the reaction of substrates with exchanged substituents furnished the same product in a good isolated yield of 74%.

In addition to the conventional characterization by spectroscopic methods, the molecular structures of **9i**,**m**,**mm** were determined using single-crystal X-ray diffraction analysis. Figure 9 illustrates the crystal structure of benzophenone **9i**. The compound crystallized in a disordered manner, with fluorine atoms seemingly occupying both para positions. This result, however, is in line with the generally accepted and frequently applied concept of isosteric replacements.[47] In the solid state, the benzene rings in **9i** are mutually twisted by 51.5(1)°, presumably to avoid possible spatial interactions of the hydrogen atoms in the ortho positions. This feature and the C═O bond length (1.234(3) Å) are similar to those observed for unsubstituted benzophenone.[48]

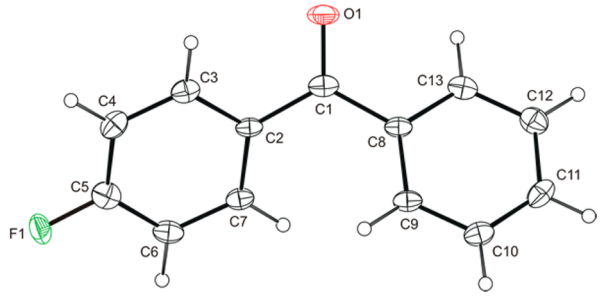

Figure 9. PLATON plot of the molecular structure of **9i** (30% probability ellipsoids). For clarity, only one position of the disordered fluorine atom is shown. Selected distances and angles (in Å and deg): C1−O1 1.234(3), C1−C2 1.486(3), C1−C8 1.491(3), C2−C1−C8 122.4(2); C5−F1 1.294(4)/C11−F2 1.298(4).

The overall structure of compound **9m** (Figure 10) is similar to that of **9i**. Like **9i**, the molecule of **9m** is twisted at the central C═O moiety, with a dihedral angle of the phenyl planes of 50.04(8)°. In contrast, the attached nitro group is nearly coplanar with the plane of its bonding aromatic ring (dihedral angle 5.4(2)°). The individual molecules in the crystal structure of **9m** assemble into stacks constituted by exactly parallel molecules, spaced out at the distance of the elemental translation along the crystallographic *a* axis ($\pi-\pi$ stacking).

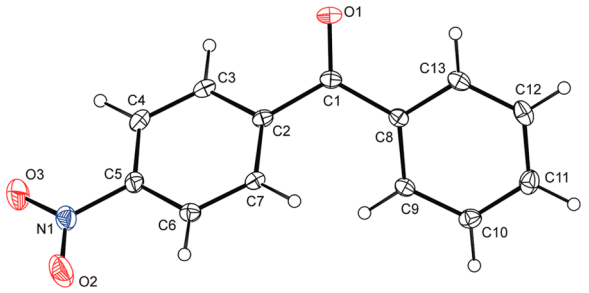

Figure 10. PLATON plot of the molecular structure of **9m** (30% probability ellipsoids). Selected distances and angles (in Å and deg): C1−O1 1.225(2), C1−C2 1.499(2), C1−C8 1.488(2), C2−C1−C8 121.0(1); N1−O2 1.222(2), N1−O3 1.215(2), O2−N1−O3 123.4(2).

Compound **9mm** crystallized with the symmetry of the chiral orthorhombic space group *Fdd*2 with half of the molecule in the asymmetric unit (Figure 11). The previous structure determination[49] for this compound led to the triclinic space group $P\bar{1}$ and two complete molecules per asymmetric unit. The molecular geometry of **9mm** is unexceptional in view of the parameters discussed above. Similar to the case for its mononitro-substituted counterpart **9m**, the molecule of **9mm** is twisted with a dihedral angle of the phenyl ring planes being 50.80(4)°. The nitro substituent remains in the plane of its parent aromatic ring (dihedral angle 4.8(2)°), and the C═O bond length is 1.218(3) Å.

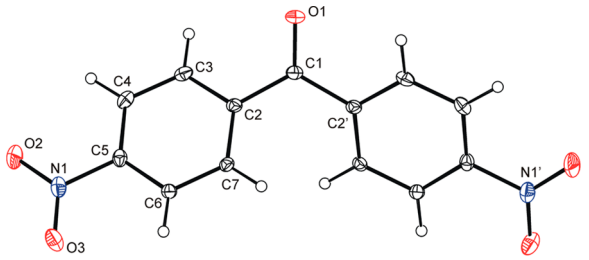

Figure 11. PLATON plot of the molecular structure of **9mm** (30% probability ellipsoids). The atoms labeled with a prime are generated by the $^1/_2 - x$, $^1/_2 - y$, z symmetry operation. Selected distances and angles (in Å and deg): C1−O1 1.218(3), C2−C1−C2′ 121.2(1), N1−O2 1.214(2), N1−O3 1.211(2), O2−N1−O3 122.9(1).

dx.doi.org/10.1021/om5006758 | *Organometallics* 2014, 33, 4131−4147

CONCLUSION

Compounds **1a**–**e** represent novel entries among the still innumerous phosphinourea donors. Because the synthesis of **1**-type ligands employs preformed building blocks that can be efficiently coupled via conventional amide coupling methods, libraries of compounds that differ in the substitution at the urea unit and, in general, also in the phosphinocarbonyl moiety and the linker connecting the amide and urea moieties are easily accessible. Ligands **1** combining extended hydrophilic and bulky lipophilic parts form extensive hydrogen-bonded assemblies in the solid state and, owing to their highly polar nature, can be employed for the preparation of catalysts suitable for use in organic solvent/water biphasic mixtures.

The defined and air-stable precatalysts of the type [PdCl(η^3-C_3H_5)(**1**-κP)] were demonstrated to efficiently catalyze the cross-coupling of boronic acids and acyl halides to give ketones. The reaction proceeds cleanly and rapidly with aromatic substrates (even at a "preparative" scale) to afford specifically substituted benzophenones in good to excellent yields at low metal loading (0.2 mol % of Pd) and under moderate reaction conditions (50 °C/1 h), with the possibility for further optimization. Importantly, the problems typically associated with poorly soluble substrates can be at least partially circumvented with the proper selection of reaction substrates, particularly through exchanging the substituents of both reaction partners. This approach enables the reasonably efficient preparation of mixed aliphatic–aromatic ketones via the coupling of saturated aliphatic acyl chlorides with aromatic boronic acids, while the formally inverted reaction of aliphatic boronic acids and aromatic acyl halides proceeds only with unsaturated boronic acids. Notably, the catalytic activity of [PdCl(η^3-C_3H_5)(**1**-κP)], expressed in turnover numbers (TONs), is relatively high for this coupling type. For instance, the 96–97% yields of **9i**, achieved at 50 °C and at room temperature with 0.2 mol % of **5e**, correspond to approximately 480 TONs, while the yield obtained at a practical 0.1 mol % catalyst loading (91%) corresponds to 910 TONs (see the Supporting Information, Table S2). These values are significantly higher than those achieved with ortho-palladated ferrocenylimines (TONs ≈ 160 for the coupling of **7a** with **8i**)[50] and some $PdCl_2$-bis(carbene) complexes (TONs ≈ 100 for the same reaction).[51]

EXPERIMENTAL SECTION

Materials and Methods. If not otherwise stated, all manipulations were performed under an argon atmosphere and away from direct sunlight, using standard Schlenk techniques. Hdpf,[6] $Ph_2PfcCONH_2$,[52] and $[(L^{NC})PdCl_2]_2$[53] were prepared according to literature procedures. Acetic anhydride, acetyl chloride, and *N*,*N*-dimethylcarbamoyl chloride were distilled under argon. Triethylamine and toluene were dried over calcium hydride and distilled under argon, while acetone was distilled from anhydrous potassium carbonate. Dichloromethane was dried with a PureSolv MD5 Solvent Purification System. Other chemicals and solvents utilized during workup, crystallization, and chromatography were used without any additional purification (chemicals, Alfa-Aesar and Sigma-Aldrich; solvents, Lachner).

NMR spectra were recorded on a Varian UNITY Inova 400 spectrometer (^{1}H, 399.95 MHz; ^{13}C, 100.58 MHz; ^{31}P, 161.90 MHz) at 25 °C. Chemical shifts (δ/ppm) are given relative to either internal tetramethylsilane (for ^{1}H and ^{13}C NMR spectra) or external 85% aqueous H_3PO_4 (for ^{31}P NMR spectra), all of which are set to 0 ppm. In addition to the standard notation of signal multiplicity, vt and vq are used to distinguish virtual triplets and quartets arising from the AA′BB′ (C_5H_4CO) and AA′BB′X ($C_5H_4PPh_2$; A, B = ^{1}H, X = ^{31}P) spin systems, constituted by protons at the substituted cyclopentadienyl rings (fc = ferrocene-1,1′-diyl). IR spectra in the range 400–4000 cm^{-1} were recorded with an FT IR instrument. Conventional low-resolution ESI-MS spectra were recorded for samples dissolved in HPLC-grade methanol. Elemental analyses were determined by the standard combustion method. In the cases where the residual solvent was present in the bulk samples, its presence and amount were verified by ^{1}H NMR analysis, and the amount of clathrated solvent was taken into account in all subsequent experiments.

Preparation of Protected Intermediates 3. *Compound **3a**.* The synthesis of acetamidocarbamate **3a** was modified from a previous report.[54] N-Boc-1,2-diaminoethane (**2b**; 2.00 g, 12.5 mmol) was dissolved in dichloromethane (50 mL), and the solution was successively treated with triethylamine (2.1 mL, 15 mmol) and acetic anhydride (1.4 mL, 15 mmol). The resulting mixture was stirred at room temperature overnight; the reaction was then terminated by the addition of 3 M HCl (50 mL). The organic phase was separated, washed with saturated aqueous $NaHCO_3$ and brine (50 mL each), and dried over anhydrous magnesium sulfate. Subsequent evaporation under vacuum afforded pure **3a** as a white powder (0.796 g, 32%).

^{1}H NMR (DMSO): δ 1.38 (s, 9 H, $C(CH_3)_3$), 1.78 (s, 3 H, CH_3CO), 2.92–2.99 (m, 2 H, CH_2), 3.00–3.07 (m, 2 H, CH_2), 6.77 (t, $^3J_{HH}$ = 5.7 Hz, 1 H, NH), 7.83 (br s, 1 H, NH). ^{13}C{^{1}H} NMR (DMSO): δ 22.52 (s, 1 C, CH_3CO), 28.13 (s, 3 C, $C(CH_3)_3$), 38.61 (s, 1 C, CH_2), 77.53 (s, 1 C, $C(CH_3)_3$), 155.51 (s, 1 C, OC(O)NH), 169.19 (s, 1 C, NHC(O)CH_3). The ^{13}C NMR signal due to the other CH_2 group is most likely obscured by the solvent resonance. IR (Nujol, cm^{-1}): ν 3351 s, 3320 s, 1684 s, 1655 s, 1530 s, 1323 m, 1281 s, 1253 w, 1238 w, 1169 s, 1100 w, 1041 w, 995 w, 976 m, 908 w, 866 m, 783 m, 768 w, 650 m, 604 m, 557 w, 481 w, 431 w. ESI+ MS: *m*/*z* 225 ([M + Na]$^+$), 241 ([M + K]$^+$), 427 ([M_2Na]$^+$). Anal. Calcd for $C_9H_{18}N_2O_3$ (202.25): C, 53.44; H, 8.97; N, 13.85. Found: C, 53.67; H, 9.04; N, 13.37. The NMR data are in agreement with the literature.[54]

*Compound **3c**.* A solution of ethyl isocyanate (0.99 mL, 12.5 mmol) in dichloromethane (15 mL) was introduced to **2b** dissolved in the same solvent (2.00 g, 12.5 mmol in 35 mL), while the mixture was stirred and cooled on ice. A white solid began to precipitate before the addition was completed. The reaction mixture was stirred at room temperature overnight and was then precipitated with hexanes (ca. 100 mL). The separated solid was filtered off, washed with hexanes, and dried under vacuum to afford **3c** as a white solid (2.42 g, 84%).

^{1}H NMR (DMSO): δ 0.97 (t, $^3J_{HH}$ = 7.2 Hz, 3 H, CH_2CH_3), 1.37 (s, 9 H, $C(CH_3)_3$), 2.89–2.96 (m, 2 H, CH_2CH_2), 2.96–3.04 (m, 4 H, CH_2CH_2 and CH_2CH_3), 5.83 (m, 2 H, NH), 6.76 (t, $^3J_{HH}$ = 4.9 Hz, 1 H, NH). ^{13}C{^{1}H} NMR (DMSO): δ 15.54 (s, 1 C, CH_2CH_3) 28.14 (s, 3 C, $C(CH_3)_3$), 33.99 (s, 1 C, CH_2), 40.76 (s, 1 C, CH_2), 77.45 (s, 1 C, $C(CH_3)_3$), 155.54 (s, 1 C, OC(O)NH), 157.94 (s, 1 C, NHC(O)NH). One signal due to the CH_2 group most likely overlaps with the solvent resonance. IR (Nujol, cm^{-1}): ν 3402 s, 3259 s, 3064 m, 3006 w, 1704 m, 1660 s, 1568 s, 1512 w, 1449 m, 1361 m, 1322 m, 1292 s, 1266 s, 1243 s, 1178 s, 1150 m, 1131 w, 1061 m, 1037 w, 986 m, 956 m, 908 w, 876 m, 766 m, 727 m, 583 br m, 519 m, 432 w. ESI+ MS: *m*/*z* 254 ([M + Na]$^+$). Anal. Calcd for $C_{10}H_{21}N_3O_3$·0.1CH_2Cl_2 (239.79): C, 50.59; H, 8.91; N, 17.53. Found: C, 51.00; H, 8.88; N, 17.80.

*Compound **3d**.* A mixture of *N*,*N*-dimethylcarbamoyl chloride (0.87 mL, 9.5 mmol), triethylamine (1.8 mL, 13 mmol), and dichloromethane (20 mL) was introduced to an ice-cold solution of **2b** (1.60 g, 10.0 mmol) in dichloromethane (30 mL) with continuous stirring, and the resultant mixture was stirred at room temperature overnight. The reaction mixture was washed with 10% NaOH (4 × 50 mL) and brine, and the organic layer was dried over magnesium sulfate and evaporated under a vacuum to afford **3d** as a white solid (2.16 g, 94%).

^{1}H NMR (DMSO): δ 1.38 (s, 9 H, $C(CH_3)_3$), 2.76 (s, 6 H, $N(CH_3)_2$), 2.92–3.00 (m, 2 H, CH_2), 3.00–3.07 (m, 2 H, CH_2), 6.28 (t, $^3J_{HH}$ = 5.2 Hz, 1 H, NH), 6.80 (t, $^3J_{HH}$ = 5.2 Hz, 1 H, NH). ^{13}C{^{1}H} NMR (DMSO): δ 28.14 (s, 3 C, $C(CH_3)_3$), 35.70 (s, 2 C,

dx.doi.org/10.1021/om5006758 | *Organometallics* 2014, 33, 4131–4147

$N(CH_3)_2$), 40.30 (s, 1 C, CH_2), 40.51 (s, 1 C, CH_2), 77.45 (s, 1 C, $C(CH_3)_3$), 155.64 (s, 1 C, NHC(O)N), 158.14 (s, 1 C, OC(O)NH). IR (Nujol, cm^{-1}): ν 3396 s, 3289 s, 1694 s, 1644 s, 1538 s, 1446 s, 1366 s, 1317 s, 1289 s, 1244 s, 1222 s, 1174 s, 1153 w, 1066 w, 1037 w, 991 s, 967 s, 878 m, 852 m, 768 m, 758 m, 720 m, 691 m, 595 w, 566 m, 529 m, 459 w. ESI+ MS: m/z 254 ($[M + Na]^+$), 270 ($[M + K]^+$), 155 ($[M - Boc + H + Na]^+$). Anal. Calcd for $C_{10}H_{21}N_3O_3$ (231.30): C, 51.90; H, 9.15; N, 18.17. Found: C, 52.00; H, 9.34; N, 18.07.

Compound ***3e***.[55] A solution of phenyl isocyanate (1.4 mL, 12.5 mmol) in dichloromethane (15 mL) was added to a solution of **2b** in the same solvent (2.0 g, 12.5 mmol in 40 mL), while the mixture was stirred and cooled on ice. A white precipitate formed immediately (N.B.: the precipitate partially dissolved upon warming to room temperature). The reaction mixture was stirred at room temperature overnight and then precipitated by the addition of hexanes (ca. 100 mL). The separated solid was filtered off, washed with hexanes, and dried under vacuum to afford **3e** as a white solid (3.28 g, 94%).

^{1}H NMR (DMSO): δ 1.38 (s, 9 H, $C(CH_3)_3$), 3.00 (br q, $^3J_{HH} \approx$ 6.0 Hz, 2 H, CH_2), 3.12 (br q, $^3J_{HH} \approx$ 6.0 Hz, 2 H, CH_2), 6.15 (t, $^3J_{HH}$ = 5.4 Hz, 1 H, NH), 6.83 (t, $^3J_{HH}$ = 5.1 Hz, 1 H, NH), 6.84–6.91 (m, 1 H, NH*Ph*), 7.18–7.24 (m, 2 H, NH*Ph*), 7.36–7.40 (m, 2 H, NH*Ph*), 8.51 (s, 1 H, NH). ^{13}C{^{1}H} NMR (DMSO): δ 28.14 (s, 3 C, $C(CH_3)_3$), 38.91 (s, 1 C, CH_2), 40.35 (s, 1 C, CH_2), 77.53 (s, 1 C, $C(CH_3)_3$), 117.53 (s, 2 C, CH NHPh), 120.88 (s, 1 C, CH^{para} NHPh), 128.51 (s, 2 C, CH NHPh), 140.42 (s, 1 C, C^{ipso} NHPh), 155.18 (s, 1 C, OC(O)NH), 155.61 (s, 1 C, NHC(O)NH). IR (Nujol, cm^{-1}): ν 3327 s, 3052 w, 1680 s, 1644 s, 1599 m, 1546 s 1499 m, 1367 m, 1322 m, 1282 m, 1258 w, 1172 s, 1137 w, 1075 w, 1027 w, 993 w 965 m, 905 w, 872 m, 856 w, 806 w, 756 m, 695 m, 671 m, 563 w, 504 m, 469 w. ESI+ MS: m/z 302 ($[M + Na]^+$), 318 ($[M + K]^+$), 581 ($[M_2Na]^+$). Anal. Calcd for $C_{14}H_{21}N_3O_3$ (279.34): C, 60.19; H, 7.58; N, 15.05. Found: C, 60.21; H, 7.38; N, 14.88.

Synthesis of the Functional Amine Hydrochlorides 4a,c–e: General Procedure.[56] A 250 mL three-necked round-bottom flask equipped with a gas inlet, gas outlet, and stir bar was charged with the corresponding protected amine **3**. The solid educt was dissolved in acetone, and the resultant solution was saturated with hydrogen chloride, generated by the addition of concentrated sulfuric acid to solid ammonium chloride and passed through concentrated H_2SO_4, at which time the solution first became turbid and then produced a white solid. After bubbling with HCl for ca. 1 h, the gas flow was interrupted, and the reaction mixture was allowed to stand for another 1 h before the separated solid was filtered off and dried under vacuum.

Compound ***4a***. The reaction of **3a** (0.680 g, 3.36 mmol) in 40 mL of acetone afforded **4a** as a white hygroscopic solid in a virtually quantitative yield (0.460 g, 99%). ^{1}H NMR (DMSO): δ 1.84 (s, 3 H, CH_3CO), 2.84 (dt, $^3J_{HH}$ = 6.0 Hz, 2 H, CH_2), 3.29 (q, $^3J_{HH}$ = 6.0 Hz, 2 H, CH_2), 8.22 (s, 1 H, NH), 8.28–8.34 (m, 1 H, NH). ^{13}C{^{1}H} NMR (DMSO): δ 22.51 (s, 1 C, CH_3CO), 36.29 (s, 1 C, CH_2), 38.39 (s, 1 C, CH_2), 169.84 (s, 1 C, $NHC(O)CH_3$). IR (Nujol, cm^{-1}): ν 3100 br s, 1591 s, 1516 m, 1323 w, 1170 s, 1106 w, 1014 m, 962 s, 777 s, 606 s, 510 m. ESI+ MS: m/z 103 ($[M - Cl]^+$). HR MS (ESI): calcd for $C_4H_{11}N_2O$ ($[M - Cl]^+$) 103.0866, found 103.0865.

Compound ***4c***.[57] The (ethylamino)carbonyl derivative **4c** was prepared as described above, starting from **3c** (2.31 g, 9.0 mmol) in 100 mL of acetone, and isolated as a white solid (1.65 g, 99%). ^{1}H NMR (DMSO): δ 1.00 (t, $^3J_{HH}$ = 7.2 Hz, 3 H, CH_2CH_3), 2.81 (tq, $^3J_{HH}$ = 6.0, 6.0 Hz, 2 H, CH_2CH_2), 3.03 (q, $^3J_{HH}$ = 7.2 Hz, 2 H, CH_2CH_3), 3.24 (t, $^3J_{HH}$ = 6.2 Hz, 2 H, CH_2CH_2), 8.22 (br s, 5 H, NH). ^{13}C{^{1}H} NMR (DMSO): δ 15.39 (s, 1 C, CH_2CH_3), 34.12 (s, 1 C, CH_2), 37.28 (s, 1 C, CH_2), 158.38 (s, 1 C, NHC(O)NH). One CH_2 resonance is most likely obscured by the solvent signal. ESI+ MS: m/z 132 ($[M - Cl]^+$). HR MS: calcd for $C_5H_{14}N_3O$ ($[M - Cl]^+$) 132.1131, found 132.1130.

Compound ***4d***. *N*-[(Dimethylamino)carbonyl]-1,2-diaminoethane hydrochloride (**4d**) was similarly obtained from **3d** (2.08 g, 10.0 mmol) in acetone (100 mL) and isolated as a white, strongly hygroscopic solid (1.46 g, 97%). ^{1}H NMR (DMSO): δ 2.81 (s, 6 H, $N(CH_3)_2$), 2.81–2.88 (m, 2 H, CH_2), 3.26 (t, $^3J_{HH}$ = 6.0 Hz, 2 H, CH_2), 7.10–7.80 (br s, 1 H, NH), 8.18 (s, 3 H, NH_3^+). ^{13}C{^{1}H} NMR (DMSO): δ 35.82 (s, 2 C, $N(CH_3)_2$), 37.97 (s, 1 C, CH_2), 39.31 (s, 1 C, CH_2), 158.24 (s, 1 C, NHC(O)N). ESI+ MS: m/z 132 ($[M - Cl]^+$), 154 ($[M - HCl + Na]^+$). HR MS: calcd for $C_5H_{14}N_3O$ ($[M - Cl]^+$) 132.1131, found 132.1129.

Compound ***4e***.[58] *N*-[(Phenylamino)carbonyl]-1,2-diaminoethane hydrochloride (**4e**) was obtained according to the general procedure from **3e** (3.27 g, 11.7 mmol) in 100 mL of acetone, resulting in a white solid (2.46 g, 98%). ^{1}H NMR (DMSO): δ 2.88 (br s, 2 H, CH_2), 3.34 (q, $^3J_{HH}$ = 6.1 Hz, 2 H, CH_2), 6.71–6.76 (m, 1 H, NH), 6.87–6.92 (m, 1 H, Ph), 7.19–7.25 (m, 2 H, Ph), 7.40–7.44 (m, 2 H, Ph), 8.06 (s, 3 H, NH_3^+), 9.11 (s, 1 H, NH). ^{13}C{^{1}H} NMR (DMSO): δ 37.00 (s, 1 C, CH_2), 39.15 (s, 1 C, CH_2), 117.61 (s, 2 C, CH Ph), 121.02 (s, 1 C, CH^{para} Ph), 128.48 (s, 2 C, CH Ph), 140.29 (s, 1 C, C^{ipso} Ph), 155.68 (s, 1 C, NHC(O)NH). IR (Nujol, cm^{-1}): ν 3327 s, 3233 s, 1659 s, 1659 s, 1596 s, 1555 m, 1526 w, 1500 m, 1438 w, 1426 m, 1318 m, 1304 m, 1241 s, 1173 m, 1129 m, 1094 m, 1079 w, 1054 m, 966 m, 912 m, 874 m, 834 w, 765 s, 738 s, 693 s, 649 br m, 607 w, 573 br m, 512 m, 504 m. ESI+ MS: m/z 180 ($[M - Cl]^+$), 202 ($[M + Na - HCl]^+$). HR MS (ESI): calcd for $C_9H_{14}N_3O$ ($[M - Cl]^+$) 180.1131, found 180.1126. Anal. Calcd for $C_9H_{14}ClN_3O$ (215.68): C, 50.12; H, 6.54; N, 19.49. Found: C, 50.13; H, 6.47; N, 19.27.

Preparation of 4b. *N*-(Aminocarbonyl)-1,2-diaminoethane hydrochloride (**4b**) was prepared directly from 1,2-diaminoethane (**2a**) according to the patent literature.[18] In our hands, however, the procedure afforded inseparable mixtures[59] of **4b** and **2a**·2HCl in varying ratios. Fortunately, the presence of **2a**·2HCl (in minor quantities with respect to **4b**) did not hamper the subsequent amidation step, leading to the desired amide **1b**.

A round-bottom flask was charged with a stir bar and diamine **2a** (6.01 g, 0.10 mol) and was equipped with a reflux condenser. Water (50 mL), sodium cyanate (7.48 g, 0.11 mol), and concentrated HCl (8.8 mL 35%, 0.10 mol) were successively added. The resulting clear solution was heated at 60 °C for 2 h. The reaction mixture was cooled and evaporated under vacuum, affording a white solid residue that was extracted with absolute ethanol (ca. 400 mL, in several portions) under sonication. The extract was evaporated under vacuum, the resulting yellowish oil was redissolved in water (50 mL), and the solution was again evaporated. The residue was then taken up in water (25 mL) and mixed with 5 M HCl (60 mL, 0.30 mol). Finally, the solution was evaporated under vacuum to afford a mixture of **4b** and **2a**·2HCl as a white solid (ca. 17 g).

^{1}H NMR (DMSO): δ 2.80 (t, $^3J_{HH}$ = 6.3 Hz, 2 H, CH_2N^+ of **4b**), 3.20 (q, $^3J_{HH} \approx$ 6.1 Hz, 2 H, $CONHCH_2$ of **4b**), 3.37 (br s, 4 H, CH_2 of **2a**·2HCl), 5.76 (br s, 6 H, NH_3 of **2a**·2HCl), 6.48 (t, $^3J_{HH} \approx$ 5.7 Hz, 1 H, $CONHCH_2$ of **4b**), 8.16 (br s, 3 H, $^+NH_3$ of **4b**). ^{13}C{^{1}H} NMR (DMSO): δ 36.49 (s, CH_2 of **2a**·2HCl), 37.30 and 39.63 (2× s, 1 C, CH_2 of **4b**), 159.33 (s, 1 C, C=O of **4b**). The **4b**:**2a**·2HCl molar ratio, determined from the NMR spectra, was ca. 8:2. Assignment of the NMR signals was corroborated by a comparison with the spectrum of an authentic sample of **2a**·2HCl.[60] ESI+ MS: m/z 229 ($[(NH_2CONHCH_2CH_2NH_2)_2Na]^+$), 207 ($[(NH_2CONHCH_2CH_2NH_2)_2H]^+$), 104 ($[\mathbf{4b} - Cl]^+$), 87 (probably $[\mathbf{4b} - Cl - NH_3]^+$).

Synthesis of Phosphinoferrocene Amides 1a–e: General Procedure. A reaction flask (A) was equipped with a stir bar, charged with Hdpf and 1-hydroxybenzotriazole (HOBt), flushed with argon, and sealed. Dichloromethane was then introduced, and the mixture containing undissolved HOBt was cooled on ice. Neat 1-ethyl-3-[3-(dimethylamino)propyl]carbodiimide (EDC) was then introduced, and the mixture was stirred for 15 min to allow the solids to completely dissolve.

In a separate flask (B), the respective hydrochloride **4** was suspended in dichloromethane, and the suspension was treated with triethylamine under sonication (ca. 5 min). The resulting mixture was transferred via cannula to flask A, and the resulting reaction mixture was stirred at room temperature overnight. The reaction mixture was first washed with 10% aqueous citric acid (3 × 100 mL) and then with saturated aqueous $NaHCO_3$ and brine (100 mL each), dried with anhydrous $MgSO_4$, and evaporated under vacuum. The residue was purified by chromatography over a silica gel column, using

dx.doi.org/10.1021/om5006758 | *Organometallics* 2014, 33, 4131–4147

dichloromethane−methanol mixtures as the eluent. Pure amides **1a−e** were isolated by evaporation and dried under vacuum.

Compound ***1a***. The general procedure mentioned above was followed, starting with Hdpf (0.872 g, 2.11 mmol), HOBt (0.427 g, 3.16 mmol), and EDC (0.55 mL, 3.16 mmol) in 60 mL of dichloromethane and **4a** (0.430 g, 3.16 mmol) and triethylamine (0.59 mL, 4.2 mmol) in 40 mL of dichloromethane. The crude product was purified by chromatography with dichloromethane−methanol at a 20:1 ratio, affording **1a** as an orange solid (0.994 g, 95%).

^{1}H NMR (DMSO): δ 1.81 (s, 3 H, CH_3CO), 3.13−3.24 (m, 4 H, CH_2), 4.05 (vq, J' = 1.8 Hz, 2 H, fc), 4.13 (vt, J' = 1.9 Hz, 2 H, fc), 4.37 (vt, J' = 1.8 Hz, 2 H, fc), 4.69 (vt, J' = 1.9 Hz, 2 H, fc), 7.27−7.33 (m, 4 H, PPh_2), 7.34−7.40 (m, 6 H, PPh_2), 7.84 (t, $^3J_{HH}$ = 5.3 Hz, 1 H, NH), 7.92 (t, $^3J_{HH}$ = 5.3 Hz, 1 H, NH). ^{13}C{^{1}H} NMR (DMSO): δ 22.56 (s, 1 C, CH_3CO), 38.49 (s, 1 C, CH_2), 38.62 (s, 1 C, CH_2), 68.86 (s, 2 C, CH fc), 71.10 (s, 2 C, CH fc), 72.79 (d, J_{PC} = 4 Hz, 2 C, CH fc), 73.43 (d, J_{PC} = 14 Hz, 2 C, CH fc), 76.58 (d, J_{PC} = 9 Hz, 1 C, *C*−P fc), 77.25 (s, 1 C, *C*−CO fc), 128.21 (d, $^3J_{PC}$ = 7 Hz, 4 C, CH^{meta} PPh_2), 128.55 (s, 2 C, CH^{para} PPh_2), 132.92 (d, $^2J_{PC}$ = 20 Hz, 4 C, CH^{ortho} PPh_2), 138.27 (d, $^1J_{PC}$ = 11 Hz, 2 C, C^{ipso} PPh_2), 168.35 (s, 1 C, $NHC(O)CH_3$), 169.38 (s, 1 C, fc*C*(O)NH). ^{31}P{^{1}H} NMR (DMSO): δ −18.2 (s). IR (Nujol, cm^{-1}): ν 3284 br m, 3089 m, 1953 w, 1824 w, 1636 s, 1552 s, 1320 m, 1293 s, 1240 s, 1197 m, 1159 m, 1096 m, 1067 w, 1059 m, 1029 m, 1021 w, 1016 w, 974 w, 933 m, 900 m, 870 w, 843 w, 834 s, 819 s, 740 s, 698 s, 660 w, 634 w, 612 m, 596 w, 588 w, 549 m, 524 m, 511 s, 485 s, 473 w, 452 s, 420 s. ESI+ MS: *m*/*z* 499 ([M + H]$^+$), 521 ([M + Na]$^+$), 537 ([M + K]$^+$). HR MS (ESI): calcd for $C_{27}H_{27}FeN_2NaO_2P$ ([M + Na]$^+$) 521.1052, found 521.1049. Anal. Calcd for $C_{27}H_{27}FeN_2O_2P{\cdot}0.2CH_2Cl_2$ (515.31): C, 63.39; H, 5.36; N, 5.44. Found: C, 63.57; H, 5.30; N, 5.32.

Compound ***1c***. The above procedure was followed using Hdpf (0.207 g, 0.50 mmol), HOBt (0.081 g, 0.60 mmol), and EDC (0.11 mL, 0.60 mmol) in 15 mL of dichloromethane and **4c** (0.101 g, 0.60 mmol) and NEt_3 (0.14 mL, 1.0 mmol) in 15 mL of dichloromethane. The reaction mixture was stirred for 5 h, and the organic phase was washed with 25 mL of each washing agent. The crude product was preadsorbed onto silica gel, and dichloromethane−methanol at a 20:1 ratio was used during column chromatography. Some unreacted Hdpf eluted first, followed by a major band of the product. Yield of **1c**: 0.212 g (80%), orange solid.

^{1}H NMR (DMSO): δ 0.97 (t, $^3J_{HH}$ = 7.2 Hz, 3 H, CH_2CH_3), 3.00 (dq, $^3J_{HH}$ = 7.2, 5.6 Hz, 2 H, CH_2CH_3), 3.10−3.21 (m, 4 H, CH_2), 4.06 (vq, J' = 1.8 Hz, 2 H, fc), 4.12 (vt, J' = 1.9 Hz, 2 H, fc), 4.37 (vt, J' = 1.7 Hz, 2 H, fc), 4.68 (vt, J' = 1.9 Hz, 2 H, fc), 5.93 (t, $^3J_{HH}$ = 5.5 Hz, 2 H, NH) 7.26−7.34 (m, 4 H, PPh_2), 7.34−7.40 (m, 6 H, PPh_2), 7.88 (t, $^3J_{HH}$ = 5.0 Hz, 1 H, NH). ^{13}C{^{1}H} NMR (DMSO): δ 15.53 (s, 1 C, CH_2CH_3), 34.04 (s, 1 C, CH_2), 68.80 (s, 2 C, CH fc), 71.10 (s, 2 C, CH fc), 72.85 (d, J_{PC} = 4 Hz, 2 C, CH fc), 73.41 (d, J_{PC} = 15 Hz, 2 C, CH fc), 76.56 (d, $^1J_{PC}$ = 9 Hz, 1 C, *C*−P fc), 77.31 (s, 1 C, *C*−CO fc), 128.20 (d, $^3J_{PC}$ = 7 Hz, 4 C, CH^{meta} PPh_2), 128.54 (s, 2 C, CH^{para} PPh_2), 132.92 (d, $^2J_{PC}$ = 20 Hz, 4 C, CH^{ortho} PPh_2), 138.30 (d, $^1J_{PC}$ = 11 Hz, 2 C, C^{ipso} PPh_2), 158.23 (s, 1 C, NHC(O)NH), 168.36 (s, 1 C, fc*C*(O)NH). ^{13}C NMR signals due to the methylene groups most likely overlap with the solvent resonance. ^{31}P{^{1}H} NMR (DMSO): δ −18.1 (s). IR (Nujol, cm^{-1}): ν 3379 m, 3273 br m, 3095 w, 1658 s, 1615 s, 1557 s, 1506 w, 1433 w, 1366 w, 1348 w, 1310 s, 1288 w, 1252 w, 1236 w, 1193 m, 1160 m, 1119 m, 1096 w, 1068 m, 1029 m, 999 w, 937 m, 910 m, 887 w, 874 w, 840 m, 812 m, 769 m, 754 m, 743 s, 698 s, 639 w, 591 w, 600 w, 546 w, 510 m, 479 s, 455 m, 423 m. ESI+ MS: *m*/*z* 550 ([M + Na]$^+$). Anal. Calcd for $C_{28}H_{30}FeN_3O_2P{\cdot}0.1CH_2Cl_2$ (535.86): C, 62.98; H, 5.68; N, 7.84. Found: C, 63.05; H, 5.55; N, 7.90.

Compound ***1d***. Hdpf (0.828 g, 2.00 mmol), HOBt 0.325 g, 2.40 mmol), and EDC (0.42 mL, 2.4 mmol) in dichloromethane (60 mL) and **4d** (0.335 g, 2.40 mmol) and NEt_3 (0.56 mL, 4.0 mmol) in dichloromethane (40 mL) were reacted according to the general procedure stated previously. During column chromatography, dichloromethane−methanol was first used at a 50:1 ratio to remove two minor bands of side products and then used at a 10:1 ratio to isolate the product. Yield: 0.795 g (75%), orange solid.

^{1}H NMR (DMSO): δ 2.77 (s, 6 H, $N(CH_3)_2$), 3.13−3.19 (m, 2 H, CH_2), 3.19−3.25 (m, 2 H, CH_2), 4.04 (vq, J' = 1.9 Hz, 2 H, fc), 4.13 (vt, J' = 1.9 Hz, 2 H, fc), 4.36 (vt, J' = 1.7 Hz, 2 H, fc), 4.69 (vt, J' = 1.9 Hz, 2 H, fc), 6.42 (t, $^3J_{HH}$ = 5.1 Hz, 1 H, NH) 7.27−7.34 (m, 4 H, PPh_2), 7.34−7.41 (m, 6 H, PPh_2), 7.92 (t, $^3J_{HH}$ = 5.2 Hz, 1 H, NH). ^{13}C{^{1}H} NMR (DMSO): δ 35.74 (s, 2 C, $N(CH_3)_2$), 40.18 (s, 1 C, CH_2), 68.85 (s, 2 C, CH fc), 71.09 (s, 2 C, CH fc), 72.76 (d, J_{PC} = 4 Hz, 2 C, CH fc), 73.41 (d, J_{PC} = 15 Hz, 2 C, CH fc), 76.59 (d, $^1J_{PC}$ = 9 Hz, 1 C, *C*−P fc), 77.32 (s, 1 C, *C*−CO fc), 128.20 (d, $^3J_{PC}$ = 7 Hz, 4 C, CH^{meta} PPh_2), 128.54 (s, 2 C, CH^{para} PPh_2), 132.90 (d, $^2J_{PC}$ = 20 Hz, 4 C, CH^{ortho} PPh_2), 138.27 (d, $^1J_{PC}$ = 11 Hz, 2 C, C^{ipso} PPh_2), 158.40 (s, 1 C, NHC(O)N), 168.51 (s, 1 C, fc*C*(O)NH). One CH_2 signal appears to be obscured by the solvent resonance. ^{31}P{^{1}H} NMR (DMSO): δ −18.2 (s). IR (Nujol, cm^{-1}): 3261 br m, 3082 w, 3067 w, 1643 s, 1627 s, 1557 s, 1432 m, 1299 m, 1232 s, 1192 m, 1157 m, 1127 w, 1096 m, 1069 m, 1023 s, 990 m, 921 m, 883 m, 866 m, 835 m, 816 m, 766 w, 754 w, 741 s, 697 s, 633 w, 590 m, 570 m, 539 m, 521 m, 501 m, 491 m, 456 m, 414 m. ESI+ MS: *m*/*z* 550 ([M + Na]$^+$). Anal. Calcd for $C_{28}H_{30}FeN_3O_2P{\cdot}0.2CH_2Cl_2$ (544.37): C, 62.22; H, 5.63; N, 7.72. Found: C, 62.62; H, 5.68; N, 7.54.

Compound ***1e***. Amide **1e** was prepared according to the previously mentioned general procedure, using Hdpf (0.828 g, 2.00 mmol), HOBt (0.325 g, 2.40 mmol), and EDC (0.42 mL, 2.4 mmol) in dichloromethane (60 mL) and **4e** (0.518 g, 2.40 mmol) and NEt_3 (0.56 mL, 4.0 mmol) in dichloromethane (40 mL). Purification and column chromatography with dichloromethane−methanol at a 10:1 ratio and preadsorbed crude product gave **1e** as an orange solid (0.600 g, 52%).

^{1}H NMR (DMSO): δ 3.23−3.28 (m, 4 H, CH_2), 4.05 (vq, J' = 1.9 Hz, 2 H, fc), 4.13 (vt, J' = 1.9 Hz, 2 H, fc), 4.37 (vt, J' = 1.7 Hz, 2 H, fc), 4.71 (vt, J' = 1.9 Hz, 2 H, fc), 6.22 (t, $^3J_{HH}$ = 5.1 Hz, 1 H, NH) 6.85−6.90 (m, 1 H, NH*Ph*), 7.17−7.22 (m, 2 H, NH*Ph*), 7.26−7.32 (m, 4 H, NH*Ph*, PPh_2), 7.34−7.41 (m, 8 H, PPh_2), 7.89 (t, $^3J_{HH}$ = 5.1 Hz, 1 H, NH), 8.58 (s, 1 H, NH). ^{13}C{^{1}H} NMR (DMSO): δ 38.79 (s, 1 C, CH_2), 40.04 (s, 1 C, CH_2), 68.83 (s, 2 C, CH fc), 71.12 (s, 2 C, CH fc), 72.86 (d, J_{PC} = 4 Hz, 2 C, CH fc), 73.41 (d, J_{PC} = 15 Hz, 2 C, CH fc), 76.54 (d, $^1J_{PC}$ = 9 Hz, 1 C, *C*−P fc), 77.24 (s, 1 C, *C*−CO fc), 117.59 (s, 2 C, CH NHPh), 120.88 (s, 1 C, CH^{para} NHPh), 128.19 (d, $^3J_{PC}$ = 7 Hz, 4 C, CH^{meta} PPh_2), 128.46 (s, 2 C, CH NHPh), 128.52 (s, 2 C, CH^{para} PPh_2), 132.91 (d, $^2J_{PC}$ = 19 Hz, 4 C, CH^{ortho} PPh_2), 138.29 (d, $^1J_{PC}$ = 11 Hz, 2 C, C^{ipso} PPh_2), 140.36 (s, 1 C, C^{ipso} NHPh), 155.35 (s, 1 C, NHC(O)NH), 168.48 (s, 1 C, fc*C*(O)NH). ^{31}P{^{1}H} NMR (DMSO): δ −18.1 (s). IR (Nujol, cm^{-1}): ν 3307 br m, 3196 w, 1765 w, 1684 s, 1621 s, 1548 s, 1498 s, 1435 s, 1364 s, 1315 s, 1242 s, 1219 s, 1194 m, 1176 w, 1163 m, 1134 m, 1119 m, 1098 m, 1068 m, 1032 s, 997 w, 942 m, 917 w, 882 m, 868 m, 842 m, 814 s, 772 w, 738 s, 696 s, 636 m, 617 w, 606 m, 590 m, 569 w, 546 m, 529 m, 502 s, 489 m, 474 w, 458 s, 416 m. ESI+ MS: *m*/*z* 576 ([M + H]$^+$), 598 ([M + Na]$^+$), 614 ([M + K]$^+$). HR MS (ESI): calcd for $C_{32}H_{31}FeN_3O_2P$ ([M + H]$^+$) 576.1498, found 576.1497. Anal. Calcd for $C_{32}H_{31}FeN_3O_2P{\cdot}0.33CH_2Cl_2$ (604.44): C, 64.24; H, 5.12; N, 6.95. Found: C, 64.25; H, 5.05; N, 6.70.

Compound ***1b***. For the preparation of **1b**, the general procedure was modified due to poor solubility. Hdpf (0.207 g, 0.50 mmol), HOBt (0.081 g, 0.60 mmol), and EDC (0.11 mL, 0.60 mmol) were reacted in dichloromethane (20 mL) at 0 °C for 15 min, as described above. In a separate flask, crude **4b** (0.176 g) was dissolved in anhydrous *N*,*N*-dimethylformamide (20 mL), and the solution was treated with triethylamine (0.21 mL, 1.5 mmol). The resulting suspension was added to the Hdpf/HOBt/EDC mixture, and the reaction mixture was stirred at room temperature overnight and then evaporated under vacuum (N.B.: evaporation at higher temperatures typically resulted in partial oxidation of the phosphine group, while incomplete evaporation leaves residual *N*,*N*-dimethylformamide in the crude product, complicating phase separation in subsequent extractions). The oily residue was taken up in dichloromethane (ca. 50 mL), and the suspension was successively washed with 10% acetic acid in saturated aqueous NaCl (2 × 50 mL) and brine, resulting in a

dx.doi.org/10.1021/om5006758 | *Organometallics* 2014, 33, 4131−4147

clear solution. The organic phase was separated, dried over $MgSO_4$, and evaporated. The crude product was purified by column chromatography over silica gel using dichloromethane−-methanol at a 20:1 ratio as the eluent. The first two minor bands were discarded, and the third major band was collected and evaporated to afford **1b** as an orange solid (0.159 g, 64%).

^{1}H NMR (DMSO): δ 3.08−3.14 (m, 2 H, CH_2), 3.14−3.21 (m, 2 H, CH_2), 4.06 (vq, J' = 1.8 Hz, 2 H, fc), 4.12 (vt, J' = 1.9 Hz, 2 H, fc), 4.38 (vt, J' = 1.8 Hz, 2 H, fc), 4.68 (vt, J' = 1.9 Hz, 2 H, fc), 5.54 (s, 2 H, NH_2), 6.06 (t, $^3J_{HH}$ = 5.4 Hz, 1 H, NH), 7.27−7.34 (m, 4 H, PPh_2), 7.34−7.40 (m, 6 H, PPh_2), 7.89 (t, $^3J_{HH}$ = 5.2 Hz, 1 H, NH). $^{13}C\{^1H\}$ NMR (DMSO): δ 68.79 (s, 2 C, CH fc), 71.10 (s, 2 C, CH fc), 72.90 (d, J_{PC} = 4 Hz, 2 C, CH fc), 73.42 (d, J_{PC} = 15 Hz, 2 C, CH fc), 76.51 (d, $^1J_{PC}$ = 9 Hz, 1 C, *C*−P fc), 77.30 (s, 1 C, *C*−CO fc), 128.20 (d, $^3J_{PC}$ = 7 Hz, 4 C, CH^{meta} PPh_2), 128.53 (s, 2 C, CH^{para} PPh_2), 132.91 (d, $^2J_{PC}$ = 19 Hz, 4 C, CH^{ortho} PPh_2), 138.30 (d, $^1J_{PC}$ = 10 Hz, 2 C, C^{ipso} PPh_2), 159.03 (s, 1 C, NHC(O)NH_2), 168.33 (s, 1 C, fc*C*(O)NH). $^{31}P\{^1H\}$ NMR (DMSO): δ −18.1 (s). IR (Nujol, cm^{-1}): ν 3391 m, 3350 m, 3246 br m, 3087 w, 1676 m, 1641 m, 1606 s, 1563 s, 1432 m, 1344 w, 1313 m, 1287 w, 1251 w, 1224 w, 1191 w, 1163 m, 1129 w, 1087 w, 1066 w, 1026 m, 969 w, 932 w, 833 m, 814 w, 775 w, 743 s, 694 s, 634 m, 596 m, 557 w, 511 m, 492 s, 449 m. ESI+ MS: *m*/*z* 522 ($[M + Na]^+$). Anal. Calcd for $C_{26}H_{26}FeN_3O_2P$ (499.32): C, 62.54; H, 5.25; N, 8.42. Found: C, 62.57; H, 5.12; N, 8.25.

Synthesis of (η^3-Allyl)palladium Complexes 5a−g: General Procedure. A suspension of ligand **1** in dichloromethane was added to a stoichiometric amount of bis(μ-chloro)bis(η^3-allyl)dipalladium (solid). The resulting mixture was stirred for 30 min, whereupon the solid educt dissolved to yield an orange solution. This solution was then filtered through a poly(tetrafluoroethylene) (PTFE) syringe filter (pore size 0.45 μm) and evaporated to dryness.

Complex ***5a***. Compound **1a** (0.249 g, 0.50 mmol) and $[PdCl(\eta^3\text{-}C_3H_5)]_2$ (0.0915 g, 0.25 mmol) were reacted in 10 mL of dichloromethane. The reaction solution was not evaporated but instead layered with diethyl ether and hexanes. Subsequent crystallization by liquid-phase diffusion over several days afforded **5a** as an orange crystalline solid (0.268 g, 79%).

^{1}H NMR ($CDCl_3$): δ 2.04 (s, 3 H, CH_3CO), 2.63 (d, J_{HH} = 12.3 Hz, 1 H, allyl CH_2), 2.82 (d, J_{HH} = 5.7 Hz, 1 H, allyl CH_2), 3.46 (qi, $^3J_{HH} \approx$ 5.0 Hz, 2 H, CH_2), 3.55 (q, $^3J_{HH} \approx$ 5.5 Hz, 2 H, CH_2), 3.58 (br s, 1 H, fc), 3.80 (br s, 1 H, fc), 3.87 (dd, J = 9.7, 13.8 Hz, 1 H, allyl CH_2), 4.23 (br s, 1 H, fc), 4.26 (br s, 1 H, fc), 4.58 (br s, 2 H, fc), 4.81 (dt, J = 1.2, 7.6 Hz, 1 H, allyl CH_2), 5.04 (br s, 1 H, fc), 5.21 (br s, 1 H, fc), 5.69 (ddd, J = 7.6, 13.8, 19.0 Hz, 1 H, allyl CH), 7.01 (br s, 1 H, NH), 7.34−7.54 (m, 8 H, PPh_2), 7.74−7.86 (m, 3 H, PPh_2 and NH). $^{13}C\{^1H\}$ NMR ($CDCl_3$): δ 23.37 (s, 1 C, CH_3CO), 38.76 (s, 1 C, CH_2), 41.89 (s, 1 C, CH_2), 62.68 (s, 1 C, allyl CH_2), 70.18 (s, 1 C, CH fc), 70.32 (s, 1 C, CH fc), 71.94 (s, 1 C, CH fc), 72.00 (s, 1 C, CH fc), 73.11 (d, J_{PC} = 8 Hz, 1 C, CH fc), 73.40 (d, J_{PC} = 7 Hz, 1 C, CH fc), 74.57 (d, $^1J_{PC}$ = 46 Hz, 1 C, *C*−P fc), 74.63 (d, J_{PC} = 10 Hz, 1 C, CH fc), 77.44 (s, 1 C, *C*−CO fc), 82.02 (d, $^2J_{PC}$ = 31 Hz, 1 C, allyl CH_2), 118.88 (d, $^2J_{PC}$ = 5 Hz, 1 C, allyl CH), 128.37 (d, J_{PC} = 10 Hz, 2 C, CH PPh_2), 128.43 (d, J_{PC} = 10 Hz, 2 C, CH PPh_2), 130.05 (s, 1 C, CH^{para} PPh_2), 130.39 (s, 1 C, CH^{para} PPh_2), 132.46 (d, J_{PC} = 12 Hz, 2 C, CH PPh_2), 133.35 (d, J_{PC} = 12 Hz, 2 C, CH PPh_2), 135.60 (d, $^1J_{PC}$ = 43 Hz, 1 C, C^{ipso} PPh_2), 136.00 (d, $^1J_{PC}$ = 45 Hz, 1 C, C^{ipso} PPh_2), 170.76 (s, 1 C, NHC(O)CH_3), 170.82 (s, 1 C, fc*C*(O)NH). One of the CH fc resonances is obscured by the solvent signal. $^{31}P\{^1H\}$ NMR ($CDCl_3$): δ 11.5 (s). IR (Nujol, cm^{-1}): ν 3298 br m, 1640 s, 1538 s, 1435 w, 1288 s, 1232 m, 1177 m, 1120 w, 1097 m, 1069 m, 1031 m, 997 w, 961 w, 907 m, 874 w, 842 s, 826 s, 750 s, 797 s, 633 w, 593 m, 537 m, 514 s, 488 s, 468 s, 443 w, 437 w. ESI+ MS: *m*/*z* 645 ($[M - Cl]^+$), 521 ($[\mathbf{1a} + Na]^+$). Anal. Calcd for $C_{30}H_{32}ClFeN_2O_2PPd\cdot 0.2CH_2Cl_2$ (698.23): C, 51.95; H, 4.68; N, 4.01. Found: C, 51.70; H, 4.87; N, 3.71.

Complex ***5b***. $[PdCl(\eta^3\text{-}C_3H_5)]_2$ (18.3 mg, 0.050 mmol) and **1b** (49.9 mg, 0.10 mmol) were reacted in 2 mL of dichloromethane, as described above. Evaporation afforded **5b** as an orange solid (33.0 mg, 97%). An analytical sample was obtained by recrystallization from dichloromethane−pentane.

^{1}H NMR (DMSO-d_6): δ 3.07−3.14 (m, 3 H, CH_2 and allyl CH_2), 3.14−3.21 (m, 3 H, CH_2 and allyl CH_2), 3.82 (br s, 1 H, allyl CH_2), 4.35 (virtual d, J' = 1.5 Hz, 2 H, fc), 4.39 (vt, J' = 1.8 Hz, 2 H, fc), 4.47 (s, 2 H, fc), 4.64 (br s, 1 H, allyl CH_2), 4.81 (vt, J' = 1.9 Hz, 2 H, fc), 5.53 (s, 2 H, NH_2), 5.84 (qi, J = 10 Hz, 1 H, allyl CH), 6.04 (t, $^3J_{HH}$ = 5.4 Hz, 1 H, NH), 7.43−7.52 (m, 10 H, PPh_2), 7.92 (t, $^3J_{HH}$ = 5.4 Hz, 1 H, NH). $^{31}P\{^1H\}$ NMR (DMSO-d_6): δ 16.8 (s). IR (Nujol, cm^{-1}): ν 3437 m, 3378 m, 3188 br m, 3078 w, 1712 w, 1673 s, 1622 s, 1557 s, 1514 s, 1440 w, 1433 m, 1306 s, 1237 m, 1194 m, 1167 m, 1153 m, 1098 m, 1071 w, 1060 w, 1034 m, 1013 w, 972 w, 928 w, 843 m, 814 m, 767 m, 757 m, 746 m, 702 m, 632 m, 585 m, 541 m, 524 m, 510 w, 486 s, 471 m, 444 w, 430 m, 412 m. ESI+ MS: *m*/*z* 646 ($[M - Cl]^+$). Anal. Calcd for $C_{29}H_{31}ClFeN_3O_2PPd$ (682.24): C, 51.05; H, 4.58; N, 6.16. Found: C, 50.83; H, 4.40; N, 5.83.

Complex ***5c***. $[PdCl(\eta^3\text{-}C_3H_5)]_2$ (9.1 mg, 0.025 mmol) and **1c** (26.4 mg, 0.050 mmol) were reacted in 1.5 mL of dichloromethane, as described above. Evaporation afforded **5c** as an orange solid in a virtually quantitative yield.

^{1}H NMR ($CDCl_3$): δ 1.13 (t, $^3J_{HH}$ = 7.2 Hz, 3 H, CH_2CH_3), 2.67 (d, J_{HH} = 12.0 Hz, 1 H, allyl CH_2), 2.74 (d, $^3J_{HH}$ = 5.4 Hz, 1 H, allyl CH_2), 3.23 (dq, $^3J_{HH}$ = 5.6, 7.2 Hz, 2 H, CH_2CH_3), 3.38−3.58 (m, 4 H, CH_2), 3.65 (s, 1 H, fc), 3.82 (s, 1 H, fc), 3.88 (dd, J = 9.8, 13.9 Hz, 1 H, allyl CH_2), 4.27 (s, 2 H, fc), 4.58 (s, 1 H, fc), 4.60 (s, 1 H, fc), 4.79−4.86 (m, 2 H, allyl CH_2 and NH), 5.02 (s, 1 H, fc), 5.18 (s, 1 H, fc), 5.64−5.75 (m, 2 H, allyl CH and NH), 7.35−7.60 (m, 9 H, PPh_2 and NH), 7.72−7.80 (m, 2 H, PPh_2). $^{31}P\{^1H\}$ NMR ($CDCl_3$): δ 11.9 (s). IR (Nujol, cm^{-1}): ν 3295 br m, 1634 s, 1538 s, 1435 m, 1303 s, 1184 m, 1168 m, 1097 m, 1060 w, 1027 m, 998 w, 964 w, 916 w, 840 m, 749 m, 696 s, 629 w, 542 w, 519 m, 493 m, 468 m, 412 w. ESI+ MS: *m*/*z* 674 ($[M - Cl]^+$). Anal. Calcd for $C_{31}H_{35}ClFeN_3O_2PPd\cdot 0.33CH_2Cl_2$ (738.32): C, 50.96; H, 4.87; N, 5.69. Found: C, 50.81; H, 4.88; N, 5.31.

Complex ***5d***. $[PdCl(\eta^3\text{-}C_3H_5)]_2$ (18.3 mg, 0.050 mmol) and **1d** (52.7 mg, 0.10 mmol) were reacted in 2 mL of dichloromethane, as described above. Rather than being evaporated, the filtered reaction mixture was layered with diethyl ether and hexanes and allowed to crystallize by liquid-phase diffusion over several days. The separated solid was filtered off and dried under vacuum to give **5d** (42.2 mg, 59%) as orange microcrystals.

^{1}H NMR (DMSO): δ 2.77 (s, 6 H, $N(CH_3)_2$), 3.12−3.18 (m, 2 H, CH_2), 3.18−3.25 (m, 2 H, CH_2), 3.82 (br s, 2 H, allyl CH_2), 4.34 (m, 2 H, fc), 4.40 (vt, J' = 1.8 Hz, 2 H, fc), 4.45 (vt, J' = 1.5 Hz, 2 H, fc), 4.64 (br s, 2 H, allyl CH_2), 4.82 (vt, J' = 1.9 Hz, 2 H, fc), 5.94 (qi, J = 10.0 Hz, 1 H, allyl CH), 6.41 (t, $^3J_{HH}$ = 5.2 Hz, 1 H, NH), 7.43−7.52 (m, 10 H, PPh_2), 7.94 (t, $^3J_{HH}$ = 5.3 Hz, 1 H, NH). $^{31}P\{^1H\}$ NMR (DMSO): δ 16.8 (s). IR (Nujol, cm^{-1}): ν 3251 br m, 3085 w, 3043 w, 1823 w, 1713 w, 1627 s, 1563 w, 1538 s, 1435 m, 1386 s, 1337 m, 1302 s, 1270 m, 1240 s, 1124 m 1193 m, 1162 m, 1099 m, 1069 m, 1035 s, 998 w, 963 w, 929 m, 862 m, 841 s, 821 w, 806 m, 771 m, 753 s, 742 s, 697 s, 628 m, 608 w, 550 w, 527 s, 505 s, 471 s, 448 m, 435 m, 407 m. ESI+ MS: *m*/*z* 674 ($[M - Cl]^+$). Anal. Calcd for $C_{31}H_{35}ClFeN_3O_2PPd$ (710.29): C, 52.42; H, 4.97; N, 5.92. Found: C, 52.14; H, 5.00; N, 5.65.

Complex ***5e***. $[PdCl(\eta^3\text{-}C_3H_5)]_2$ (36.3 mg, 0.10 mmol) and **1e** (115 mg, 0.20 mmol) were reacted in 4 mL of dichloromethane, as described above. The reaction solution was filtered, layered with diethyl ether and hexanes, and set aside for crystallization, which furnished **5e** in the form of well-developed orange crystals (57.4 mg, 76%).

^{1}H NMR ($CDCl_3$): δ 2.69 (d, J = 11.8 Hz, 1 H, allyl CH_2), 2.85 (d, J = 5.5 Hz, 1 H, allyl CH_2), 3.41−3.65 (m, 4 H, CH_2), 3.64 (br s, 1 H, fc), 3.79 (br s, 1 H, fc), 3.88 (dd, J = 9.7, 13.8 Hz, 1 H, allyl CH_2), 4.27 (m, 2 H, fc), 4.55 (br s, 1 H, fc), 4.57 (br s, 1 H, fc), 4.81 (dt, J = 1.4, 7.2 Hz, 1 H, allyl CH_2), 5.04 (br s, 1 H, fc), 5.18 (br s, 1 H, fc), 5.68 (ddd, J = 7.6, 13.8, 18.9 Hz, 1 H, allyl CH), 6.16 (br s, 1 H, NH), 6.94−7.00 (m, 1 H, NH*Ph*), 7.20−7.28 (m, 3 H, NH*Ph*), 7.35−7.55 (m, 11 H, PPh_2, NH*Ph* and NH), 7.68−7.78 (m, 2 H, PPh_2). $^{31}P\{^1H\}$ NMR ($CDCl_3$): δ 12.0 (s). IR (Nujol, cm^{-1}): ν 3281 br m, 1697 s, 1615 s, 1552 s, 1497 m, 1438 m, 1306 s, 1202 m, 1189 w, 1169 m, 1134 w, 1103 m, 1074 w, 1030 m, 999 w, 973 w, 928 m, 891 w, 839 m,

dx.doi.org/10.1021/om5006758 | *Organometallics* 2014, 33, 4131−4147

823 m, 792 w, 748 s, 698 s, 668 w, 633 w, 618 w, 600 m, 534 m, 523 m, 510 m, 491 s, 463 m, 445 m, 432 m, 413 m. ESI+ MS: m/z 780 ($[M + Na]^+$), 722 ($[M - Cl]^+$), 614 ($[\mathbf{1e} + K]^+$), 598 ($[\mathbf{1e} + Na]^+$). Anal. Calcd for $C_{35}H_{35}ClFeN_3O_2PPd\cdot0.33CH_2Cl_2$ (786.36): C, 53.96; H, 4.57; N, 5.34. Found: C, 54.06; H, 4.40; N, 5.24.

*[PdCl(η^3-C_3H_5)(Hdpf-κP)] (**5f**).* [PdCl(η^3-C_3H_5)]$_2$ (91.5 mg, 0.25 mmol) and Hdpf (207 mg, 0.50 mmol) were reacted in dichloromethane (10 mL), according to the general procedure stated previously. Subsequent evaporation afforded **5f** as an orange solid in a quantitative yield.

^{1}H NMR ($CDCl_3$): δ 2.77 (d, J = 9.9 Hz, 1 H, allyl CH_2), 3.13 (bs, 1 H, allyl CH_2), 3.83 (dd, J = 10.3, 13.6 Hz, 1 H, allyl CH_2), 4.50 (vq, J' = 1.8 Hz, 2 H, fc), 4.54−4.56 (m, 2 H, fc), 4.57 (br s, 2 H, fc), 4.81 (t, J = 7.4 Hz, 1 H, allyl CH_2), 4.87 (vt, J' = 1.9 Hz, 2 H, fc), 5.57−5.67 (m, 1 H, allyl CH), 6.8 (very br s, 1 H, NH), 7.35−7.46 (m, 6 H, PPh_2), 7.45−7.62 (m, 4 H, PPh_2). ^{31}P{^{1}H} NMR ($CDCl_3$): δ 15.3 (s). IR (Nujol, cm^{-1}): ν 3400 br m, 1710 s, 1674 s, 1298 m, 1167 m, 1098 m, 1031 m, 837 m, 747 m, 696 m, 629 w, 537 m, 519 m, 504 m, 469 m. ESI+ MS: m/z 561 ($[M - Cl]^+$). Anal. Calcd for $C_{26}H_{24}O_2FePPdCl\cdot0.1CH_2Cl_2$ (605.62): C, 52.76; H, 4.19. Found: C, 52.75; H, 4.29.

*[PdCl(η^3-C_3H_5)($Ph_2PfcCONH_2$-κP)] (**5g**).* The reaction of [PdCl(η^3-C_3H_5)]$_2$ (18.3 mg, 0.05 mmol) with $Ph_2PfcCONH_2$ (41.3 mg, 0.10 mmol) in 2 mL of dichloromethane, as described above, provided complex **5g** as an orange solid in a quantitative yield.

^{1}H NMR ($CDCl_3$): δ 2.62 (d, J = 12.3 Hz, 1 H, allyl CH_2), 2.87 (d, J = 5.5 Hz, 1 H, allyl CH_2), 3.80 (dd, J = 9.9 Hz, J = 14.0 Hz, 1 H, allyl CH_2), 3.84 (br s, 1 H, fc), 3.93 (br s, 1 H, fc), 4.24 (br s, 1 H, fc), 4.28 (br s, 1 H, fc), 4.61 (br s, 1 H, fc), 4.63 (br s, 1 H, fc), 4.77 (dt, J = 1.4, 7.2 Hz, 1 H, allyl CH_2), 5.10 (br s, 1 H, fc), 5.19 (br s, 1 H, fc), 5.4 (br s, 1 H, NH), 5.59 (ddd, J = 7.3, 13.8, 19.0 Hz, 1 H, allyl CH), 7.16 (br s, 1 H, NH), 7.36−7.48 (m, 6 H, PPh_2), 7.52−7.60 (m, 2 H, PPh_2), 7.68−7.76 (m, 2 H, PPh_2). ^{31}P{^{1}H} NMR ($CDCl_3$): δ 11.9 (s). IR (Nujol, cm^{-1}): ν 3176 br m, 1655 s, 1604 m, 1308 w, 1167 m, 1098 m, 1028 m, 999 w, 910 w, 910 w, 838 m, 781 w, 747 m, 696 s, 628 w, 519 m, 502 m, 468 m. ESI+ MS: m/z 560 ($[M - Cl]^+$. Anal. Calcd for $C_{26}H_{25}ClFeNOPPd$ (596.14): C, 52.38; H, 4.23; N, 2.35. Found: C, 52.15; H, 4.12; N, 2.13.

Preparation of Pd(II) Complexes with an Auxiliary 2-[(Dimethylamino-κ*N*)methyl]phenyl-κ*C*^{1} Ligand (6a−e): General Procedure. Stoichiometric amounts of bis(μ-chloro)bis{2-[(dimethylamino-κ*N*)methyl]phenyl-κ*C*^{1}}dipalladium ([(L^{NC})PdCl]$_2$) and ligand **1** were mixed in dichloromethane. The resulting orange solution was stirred at room temperature for 30 min, filtered through a PTFE syringe filter (0.45 μm pore size), and then evaporated under vacuum to afford complex **6** in an essentially quantitative yield. The product typically tended to maintain the reaction solvent, the presence of which was verified by NMR analysis.

*Complex **6a**.* Following the aforementioned general procedure, [(L^{NC})PdCl]$_2$ (27.6 mg, 0.050 mmol) and **1a** (49.8 mg, 0.10 mmol) were reacted in dichloromethane (5 mL) to afford **6a** as an orange solid (75.8 mg, 98%).

^{1}H NMR ($CDCl_3$): δ 1.90 (s, 3 H, CH_3CO), 2.87 (d, $^4J_{PH}$ = 2.8 Hz, 6 H, $N(CH_3)_2$), 3.38−3.44 (m, 2 H, CH_2), 3.46−3.52 (m, 2 H, CH_2), 4.15 (d, $^4J_{PH}$ = 2.2 Hz, 1 H, $NCH_2C_6H_4$), 4.36 (vq, J' = 1.9 Hz, 2 H, fc), 4.42−4.45 (m, 2 H, fc), 4.60 (vt, J' = 1.9 Hz, 2 H, fc), 5.05 (br vt, J' = 1.9 Hz, 2 H, fc), 6.24 (ddd, J = 1.1, 6.6, 7.8 Hz, 1 H, C_6H_4), 6.37 (td, J = 1.2, 7.5 Hz, 1 H, C_6H_4), 6.76 (br s, 1 H, NH), 6.82 (td, J = 1.1, 7.3 Hz, 1 H, C_6H_4), 7.01 (dd, J = 1.6, 7.5 Hz, 1 H, C_6H_4), 7.29−7.35 (m, 4 H, PPh_2), 7.38−7.43 (m, 3 H, PPh_2 and NH), 7.53−7.60 (m, 4 H, PPh_2). ^{13}C{^{1}H} NMR ($CDCl_3$): δ 23.16 (s, 1 C, CH_3CO), 39.76 (s, 1 C, CH_2), 40.80 (s, 1 C, CH_2), 50.07 (d, $^3J_{PC}$ = 2 Hz, 2 C, $N(CH_3)_2$), 70.52 (s, 2 C, CH fc), 73.07 (s, 2 C, CH fc), 73.55 (d, $^3J_{PC}$ = 3 Hz, 1 C, $NCH_2C_6H_4$), 73.65 (d, J_{PC} = 7 Hz, 2 C, CH fc), 75.56 (d, $^1J_{PC}$ = 59 Hz, 1 C, *C*−P fc), 77.89 (s, 1 C, *C*−CO fc), 122.51 (s, 1 C, CH C_6H_4), 123.88 (s, 1 C, CH C_6H_4), 125.04 (d, J_{PC} = 6 Hz, 1 C, CH C_6H_4), 128.04 (d, J_{PC} = 11 Hz, 4 C, CH PPh_2), 130.68 (d, $^4J_{PC}$ = 2 Hz, 2 C, CH^{para} PPh_2), 131.47 (d, J_{PC} = 49 Hz, 2 C, C_{ipso} PPh_2), 134.36 (d, J_{PC} = 12 Hz, 4 C, CH PPh_2), 138.43 (d, J_{PC} = 11 Hz, 1 C, CH C_6H_4), 147.79 (d, J_{PC} = 2 Hz, 1 C, C^{ipso} C_6H_4), 151.98 (s, 1 C, C^{ipso} C_6H_4), 170.82 (s, 1 C, $NHC(O)CH_3$), 171.10 (s, 1 C, fc*C*(O)NH). Two resonances due to CH fc overlapped with the solvent signal. ^{31}P{^{1}H} NMR ($CDCl_3$): δ 32.9 (s). IR (Nujol, cm^{-1}): ν 3291 br m, 3050 br m, 1634 s, 1538 s, 1436 w, 1290 br m, 1183 w, 1165 m, 1099 m, 1029 m, 994 w, 972 w, 844 m, 744 s, 696 s, 628 w, 597 w, 542 w, 505 m, 477 m, 439 w. ESI+ MS: m/z 738 ($[M - Cl]^+$). Anal. Calcd for $C_{36}H_{39}ClFeN_3O_2PPd\cdot0.5CH_2Cl_2$ (816.84): C, 53.67; H, 4.94; N, 5.15. Found: C, 53.90; H, 5.07; N, 4.76.

*Complex **6b**.* Following the previously stated general procedure, [(L^{NC})PdCl]$_2$ (13.8 mg, 0.025 mmol) and **1b** (25.0 mg, 0.050 mmol) were reacted in dichloromethane (1.5 mL). The product was precipitated with pentane and isolated by centrifugation. Yield of **6b**: 37.4 mg (96%), fine orange solid.

^{1}H NMR ($CDCl_3$): δ 2.86 (d, $^4J_{PH}$ = 2.7 Hz, 6 H, $N(CH_3)_2$), 3.30−3.37 (m, 2 H, CH_2), 3.37−3.44 (m, 2 H, CH_2), 4.15 (d, $^4J_{PH}$ = 2.0 Hz, 2 H, $NCH_2C_6H_4$), 4.38−4.41 (m, 2 H, fc), 4.41−4.44 (m, 2 H, fc), 4.61 (vt, J' = 1.9 Hz, 2 H, fc), 4.8 (br s, 1 H, NH), 5.03 (vt, J' = 1.9 Hz, 2 H, fc), 6.23 (ddd, J = 1.0, 6.5, 7.7 Hz, 1 H, C_6H_4), 6.38 (td, J = 1.3, 7.6 Hz, 1 H, C_6H_4), 6.83 (td, J = 1.1, 7.4 Hz, 1 H, C_6H_4), 7.01 (dd, J = 1.5, 7.4 Hz, 1 H, C_6H_4), 7.27−7.35 (m, 4 H, PPh_2), 7.37−7.43 (m, 2 H, PPh_2), 7.45 (br s, 1 H, NH), 7.49−7.56 (m, 4 H, PPh_2). ^{31}P{^{1}H} NMR ($CDCl_3$): δ 33.0 (s). IR (Nujol, cm^{-1}): ν 3250 br w, 1635 s, 1540 s, 1435 w, 1300 m, 1238 m, 1183 m, 1164 m, 1098 m, 1060 w, 1028 m, 992 m, 972 m, 933 w, 864 w, 844 s, 773 w, 744 s, 694 s, 654 w, 628 m, 520 w, 508 s. ESI+ MS: m/z 739 ($[M - Cl]^+$). Anal. Calcd for $C_{35}H_{38}ClFeN_4O_2PPd\cdot0.5CH_2Cl_2$ (817.83): C, 52.13; H, 4.81; N, 6.85. Found: C, 52.08; H, 4.98; N, 6.57.

*Complex **6c**.* [(L^{NC})PdCl]$_2$ (13.8 mg, 0.025 mmol) and **1c** (26.4 mg, 0.050 mmol) were reacted in dichloromethane (1.5 mL), according to the general procedure, to afford **6c** (39.6 mg, quantitative) as an orange solid.

^{1}H NMR ($CDCl_3$): δ 1.01 (t, $^3J_{HH}$ = 7.3 Hz, 3 H, CH_2CH_3), 2.86 (d, $^4J_{PH}$ = 2.7 Hz, 6 H, $N(CH_3)_2$), 3.11 (dq, $^3J_{HH}$ = 5.6, 7.3 Hz, 2 H, CH_2CH_3), 3.33−3.40 (m, 2 H, CH_2), 3.40−3.47 (m, 2 H, CH_2), 4.15 (d, $^4J_{PH}$ = 1.9 Hz, 2 H, $NCH_2C_6H_4$), 4.38 (vq, J' = 1.9 Hz, 2 H, fc), 4.41−4.45 (m, 2 H, fc), 4.62 (vt, J' = 1.9 Hz, 2 H, fc), 4.88 (br s, 1 H, NH), 5.03 (vt, J' = 1.8 Hz, 2 H, fc), 5.49 (br s, 1 H, NH), 6.24 (ddd, J = 1.1, 6.5, 7.8 Hz, 1 H, C_6H_4), 6.37 (td, J = 1.5, 7.4 Hz, 1 H, C_6H_4), 6.83 (td, J = 1.1, 7.4 Hz, 1 H, C_6H_4), 7.01 (dd, J = 1.5, 7.4 Hz, 1 H, C_6H_4), 7.30−7.36 (m, 4 H, PPh_2), 7.38−7.44 (m, 2 H, PPh_2), 7.51−7.58 (m, 4 H, PPh_2). ^{31}P{^{1}H} NMR ($CDCl_3$): δ 32.8. IR (Nujol, cm^{-1}): ν 3306 m, 1634 s, 1538 s, 1436 w, 1303 m, 1182 w, 1164 m, 1098 m, 1060 w, 1028 m, 993 w, 972 w, 844 m, 743 s, 695 s, 628 m, 544 m, 521 s, 506 s, 476 m. ESI+ MS: m/z 767 ($[M - Cl]^+$). Anal. Calcd for $C_{37}H_{42}ClFeN_4O_2PPd\cdot0.2CH_2Cl_2$ (820.40): C, 54.46; H, 5.21; N, 6.83. Found: C, 54.37; H, 5.11; N, 6.62.

*Complex **6d**.* The general procedure was followed, starting with [(L^{NC})PdCl]$_2$ (27.6 mg, 0.050 mmol) and **1d** (52.7 mg, 0.10 mmol) in dichloromethane (5 mL). Evaporation provided **6d** as an orange solid (79.8 mg, quantitative).

^{1}H NMR ($CDCl_3$): δ 2.85 (s, 6 H, $C(O)N(CH_3)_2$) 2.86 (d, $^4J_{PH}$ = 2.8 Hz, 6 H, $PdN(CH_3)_2$), 3.38−3.43 (m, 2 H, CH_2), 3.43−3.49 (m, 2 H, CH_2), 4.14 (d, $^4J_{PH}$ = 2.1 Hz, 2 H, $NCH_2C_6H_4$), 4.40 (m, 4 H, fc), 4.68 (vt, J' = 1.9 Hz, 2 H, fc), 4.98 (vt, J' = 1.9 Hz, 2 H, fc), 5.4 (br s, 1 H, NH), 6.24 (ddd, J = 1.2, 6.5, 7.8 Hz, 1 H, C_6H_4), 6.37 (td, J = 1.5, 7.5 Hz, 1 H, C_6H_4), 6.82 (td, J = 1.2, 7.3 Hz, 1 H, C_6H_4), 7.01 (dd, J = 1.5, 7.4 Hz, 1 H, C_6H_4), 7.30−7.35 (m, 4 H, PPh_2), 7.38−7.44 (m, 2 H, PPh_2), ca. 7.5 (br s, 1 H, NH), 7.53−7.59 (m, 4 H, PPh_2). ^{31}P{^{1}H} NMR ($CDCl_3$): δ 32.8 (s). IR (Nujol, cm^{-1}): ν 3300 br m, 1634 s, 1537 s, 1303 m, 1183 w, 1165 m, 1099 m, 1029 m, 997 w, 845 m, 744 m, 696 m, 628 w, 544 w, 521 m, 507 m. ESI+ MS: m/z 767 ($[M - Cl]^+$). Anal. Calcd for $C_{37}H_{42}ClFeN_4O_2PPd\cdot0.33CH_2Cl_2$ (831.44): C, 53.92; H, 5.17; N, 6.74. Found: C, 53.80; H, 5.28; N, 6.31.

*Complex **6e**.* [(L^{NC})PdCl]$_2$ (27.6 mg, 0.050 mmol) and **1e** (57.5 mg, 0.10 mmol) were reacted in dichloromethane (5 mL), according to the general procedure stated previously, to give **6e** as an orange solid (84.8 mg, quantitative).

^{1}H NMR ($CDCl_3$): δ 2.84 (d, $^4J_{PH}$ = 2.7 Hz, 6 H, $N(CH_3)_2$), 3.37−3.43 (m, 2 H, CH_2), 3.43−3.49 (m, 2 H, CH_2), 4.14 (d, $^4J_{PH}$ = 2.1 Hz, 2 H, $NCH_2C_6H_4$), 4.35 (vq, J' = 1.8 Hz, 2 H, fc), 4.39−4.41 (m, 2 H,

dx.doi.org/10.1021/om5006758 | *Organometallics* 2014, 33, 4131−4147

fc), 4.58 (vt, J' = 1.9 Hz, 2 H, fc), 5.05 (vt, J' = 1.8 Hz, 2 H, fc), ca. 6.1 (br s, 1 H, NH),), 6.24 (ddd, J = 1.1, 6.6, 7.8 Hz, 1 H, C_6H_4), 6.38 (td, J = 1.5, 7.7 Hz, 1 H, C_6H_4), 6.83 (td, J = 1.1, 7.3 Hz, 1 H, C_6H_4), 6.94 (tt, J = 1.3, 7.3 Hz, 1 H, NH*Ph*), 7.01 (dd, J = 1.5, 7.4 Hz, 1 H, C_6H_4), 7.15−7.20 (m, 2 H, NH*Ph*), 7.26−7.60 (m, 15 H, PPh_2, NH*Ph* and NH). $^{31}P\{^1H\}$ NMR ($CDCl_3$): δ 32.8 (s). IR (Nujol, cm^{-1}): ν 3300 br m, 1633 s, 1596 m, 1538 s, 1497 m, 1436 w, 1310 s, 1240 br m, 1178 w, 1164 m, 1098 m, 1028 m, 993 w, 971 w, 864 w, 844 m, 743 s, 693 s, 628 w, 541 w, 505 s, 477 m, 439 w. ESI+ MS: m/z 815 ($[M - Cl]^+$). Anal. Calcd for $C_{41}H_{42}O_2N_4FePPdCl{\cdot}0.5CH_2Cl_2$ (893.92): C, 55.76; H, 4.85; N, 6.27. Found: C, 55.77; H, 4.94; N, 5.93.

Catalytic Tests. A Schlenk tube was charged (in this order) with the appropriate acyl halide (1.5 mmol), boronic acid (1.25 mmol), sodium carbonate (133 mg, 1.25 mmol), catalyst (typically 0.2 mol % Pd with respect to the boronic acid), and a stir bar and then flushed with argon and sealed with a rubber septum. Toluene (or C_6D_6 for screening experiments) and water (3 mL each) were introduced, and the reaction vessel was transferred to an oil bath maintained at 50 °C. After it was stirred for the given reaction time (typically 1 h), the reaction mixture was transferred to a separatory funnel and diluted with diethyl ether (20 mL). The aqueous phase was separated, and the organic phase was washed successively with 3 M HCl (twice), 5% KOH (four times), and brine (two times) before being dried over anhydrous magnesium sulfate and evaporated under vacuum with a chromatography-grade silica gel to allow preadsorption of the crude product. Subsequent column chromatography on silica gel with hexanes−ethyl acetate (30:1, 10:1, or 5:1 v:v) followed by evaporation afforded the analytically pure product. N.B.: results of the screening experiments performed at different reaction times and with different amounts of reagents and catalyst loading are provided in the Supporting Information (Table S2).

Preparation of **9j** on a 10 mmol scale was performed as described above using 4-chlorobenzoyl chloride (2.10 g, 12 mmol), phenylboronic acid (1.22 g, 10 mmol), sodium carbonate (1.06 g, 10 mmol), and catalyst **5e** (7.6 mg, 0.01 mmol). The reaction was performed in a toluene−water mixture (25 mL each) at 50 °C for 1 h, and subsequent chromatographic isolation afforded the analytically pure ketone in a virtually quantitative yield (2.14 g, 99%).

X-ray Crystallography. The diffraction data ($\pm h,\pm k, \pm l$, θ_{max} = 26−27.5°, completeness ≥98%) were collected with a Nonius KappaCCD diffractometer using graphite-monochromated Mo Kα radiation (λ = 0.71073 Å). During analysis, the temperature was controlled with the aid of a Cryostream Cooler (Oxford Cryosystems). The data were analyzed and corrected for absorption using the methods included in the diffractometer software. Details on data collection, structure solution, and refinement are available in the Supporting Information (Table S3).

The structures were solved using direct methods (SHELXS97[61]) and refined by full-matrix least-squares routines based on F^2 (SHELXL97[61]). All non-hydrogen atoms were refined with anisotropic displacement parameters. The hydrogen atoms residing on oxygen (OH) and nitrogen (NH) atoms were located on the difference electron density maps and refined as riding atoms with unconstrained U_{iso}(H) values (free ligands and **6a**) or with U_{iso}(H) values set to a multiple of U_{eq}(O/N) (all other complexes). The carbon-bound hydrogens were included in their calculated positions and were similarly refined. Particular details on structure treatment are as follows.

The allyl moieties in *all* (η^3-C_3H_5)Pd complexes were disordered and were thus modeled over two positions. The relative abundances of these two orientations varied from ca. 61:39 to ca. 92:8 (see also above).[27] The structure of **5c** was further complicated by disorder of the terminal ethyl group, whose methyl moiety was freely refined over two positions, with nearly 50:50 occupancies. Crystallization of compound **6a** afforded the stoichiometric solvate **6a**·$^1/_2CH_3OH{\cdot}^1/_2CH_3CO_2Et$ with extensively disordered solvent molecules that were modeled by PLATON/SQUEEZE.[62] The number of electrons calculated by SQUEEZE (126 e per unit cell) corresponded well with the number of electrons expected for two molecules of ethyl acetate and two molecules of methanol per the unit cell (132 e). Finally, the fluorine atom in the structure of **9i** was refined with equal occupancies over the two para positions (see discussion above).

Geometric calculations were performed with a recent version of the PLATON program.[63] All numerical values were rounded with respect to the estimated standard deviations (ESDs) given to one decimal place. Parameters pertaining to atoms in constrained positions (hydrogens) are given without ESDs.

■ ASSOCIATED CONTENT

Ⓢ Supporting Information

Text, figures, tables, and CIF files giving an overlap of the independent molecules in the crystal structure of **1b**, description of the crystal structures of **5f** and **5g**, results of the catalytic screening experiments, characterization data of the benzophenones **9**, crystallographic data for **1b**·CH_3OH, **1c**, **5b**,**c**,**f**,**g**, **6a**, and **9i**,**m**,**mm** and the NMR spectra of compounds **1** and **3**−**6**. This material is available free of charge via the Internet at http://pubs.acs.org.

■ AUTHOR INFORMATION

Corresponding Author

*E-mail for P.S.: stepnic@natur.cuni.cz.

Notes

The authors declare no competing financial interest.

■ ACKNOWLEDGMENTS

This work was financially supported by the Czech Science Foundation (project no. 13-08890S) and the Grant Agency of Charles University in Prague (project no. 643012).

■ REFERENCES

(1) (a) *Ferrocenes: Ligands, Materials and Biomolecules*; Štěpnička, P., Ed.; Wiley: Chichester, U.K., 2008; Part I-Ligands, pp 1−277. (b) Štěpnička, P. In *The Chemistry of Organoiron Compounds*; Marek, I., Rappoport, Z., Eds.; Wiley: Chichester, U.K., 2013; Chapter 4, pp 103−154. (c) Atkinson, R. C. J.; Gibson, V. C.; Long, N. J. *Chem. Soc. Rev.* **2004**, *33*, 313. (d) Gómez Arrayás, R.; Adrio, J.; Carretero, J. C. *Angew. Chem., Int. Ed.* **2006**, *45*, 7674.

(2) (a) Astruc, D.; Chardac, F. *Chem. Rev.* **2001**, *101*, 2991. (b) Kölner, C.; Pugin, B.; Togni, A. *J. Am. Chem. Soc.* **1998**, *120*, 10274. (c) Kölner, C.; Togni, A. *Can. J. Chem.* **2001**, *79*, 1762. For smaller dendritic donors, see: (d) Kühnert, J.; Lamač, M.; Demel, J.; Nicolai, A.; Lang, H.; Štěpnička, P. *J. Mol. Catal. A: Chem.* **2008**, *285*, 41. (e) Lamač, M.; Tauchman, J.; Dietrich, S.; Císařová, I.; Lang, H.; Štěpnička, P. *Appl. Organomet. Chem.* **2010**, *24*, 326.

(3) Selected examples: (a) Culler, W. R.; Han, N. F. *J. Organomet. Chem.* **1987**, *333*, 269. (b) Johnson, B. F. G.; Raynor, S. A.; Shephard, D. S.; Mashmeyer, T.; Thomas, J. M.; Sankar, G.; Bromley, S.; Oldroyd, R.; Gladden, L.; Mantle, M. D. *J. Chem. Soc., Chem. Commun.* **1999**, 1167. (c) Gotov, B.; Toma, Š.; Macquarrie, D. J. *Enantiomer* **1999**, *4*, 263. (d) Gotov, B.; Toma, Š.; Macquarrie, D. J. *New J. Chem.* **2000**, *24*, 597. (e) Pugin, B.; Landert, H.; Spindler, F.; Blaser, H.-U. *Adv. Synth. Catal.* **2002**, *344*, 974. (f) Cvengroš, J.; Toma, Š.; Žemberyová, M.; Macquarrie, D. J. *Molecules* **2005**, *10*, 679.

(4) (a) Pugin, B.; Landert, H. (Novartis AG, Switzerland). Functionalized ferrocenyldiphosphines, a process for their preparation and their use. International Patent WO 9801457, 1998. (b) Pugin, B. (Solvias AG, Switzerland). Diphosphine ligands for metal complexes. International Patent WO 2001004131, 2001.

(5) Štěpnička, P. *Chem. Soc. Rev.* **2012**, *41*, 4273.

(6) Podlaha, J.; Štěpnička, P.; Ludvík, J.; Císařová, I. *Organometallics* **1996**, *15*, 543.

(7) (a) Schulz, J.; Císařová, I.; Štěpnička, P. *J. Organomet. Chem.* **2009**, *694*, 2519. (b) Tauchman, J.; Císařová, I.; Štěpnička, P. *Organometallics* **2009**, *28*, 3288. (c) Tauchman, J.; Císařová, I.;

Štěpnička, P. *Eur. J. Org. Chem.* **2010**, 4276. (d) Tauchman, J.; Císařová, I.; Štěpnička, P. *Dalton Trans.* **2011**, *40*, 11748. (e) Schulz, J.; Císařová, I.; Štěpnička, P. *Organometallics* **2012**, *31*, 729. (f) Tauchman, J.; Therrien, B.; Süss-Fink, G.; Štěpnička, P. *Organometallics* **2012**, *31*, 3985. (g) Schulz, J.; Císařová, I.; Štěpnička, P. *Eur. J. Inorg. Chem.* **2012**, 5000.

(8) (a) Kühnert, J.; Dušek, M.; Demel, J.; Lang, H.; Štěpnička, P. *Dalton Trans.* **2007**, 2802. (b) Kühnert, J.; Císařová, I.; Lamač, M.; Štěpnička, P. *Dalton Trans.* **2008**, 2454. (c) Štěpnička, P.; Krupa, M.; Lamač, M.; Císařová, I. *J. Organomet. Chem.* **2009**, *694*, 2987. (d) Štěpnička, P.; Schneiderová, B.; Schulz, J.; Císařová, I. *Organometallics* **2013**, *32*, 5754. (e) Tauchman, J.; Císařová, I.; Štěpnička, P. *Dalton Trans.* **2014**, *43*, 1599.

(9) (a) Nasser, N.; Puddephatt, R. J. *Cryst. Growth Des.* **2012**, *12*, 4275. (b) Nasser, N.; Boyle, P. D.; Puddephatt, R. J. *Organometallics* **2013**, *32*, 5504. (c) Nasser, N.; Puddephatt, R. J. *Inorg. Chim. Acta* **2014**, *409*, 238.

(10) Constable, E. C.; Hostettler, N.; Housecroft, C. E.; Murray, N. S.; Schönle, J.; Soydaner, U.; Walliser, R. M.; Zampese, J. A. *Dalton Trans.* **2013**, *42*, 4970.

(11) (a) Ye, N.; Dai, W.-M. *Eur. J. Org. Chem.* **2013**, 831. (b) Philipova, I.; Stavrakov, G.; Dimitrov, V. *Tetrahedron: Asymmetry* **2012**, *23*, 927.

(12) (a) Duckmanton, P. A.; Blake, A. J.; Love, J. B. *Inorg. Chem.* **2005**, *44*, 7708. (b) Knight, L. K.; Freixa, Z.; van Leeuwen, P. W. N. M.; Reek, J. N. H. *Organometallics* **2006**, *25*, 954. (c) Meeuwissen, J.; Detz, R. J.; Sandee, A. J.; de Bruin, B.; Reek, J. N. H. *Dalton Trans.* **2010**, *39*, 1929. (d) Meeuwissen, J.; Detz, R.; Sandee, A. J.; de Bruin, B.; Siegler, M. A.; Spek, A. L.; Reek, J. N. H. *Eur. J. Inorg. Chem.* **2010**, 2992.

(13) Hayashi, T.; Mise, T.; Fukushima, M.; Kagotani, M.; Nagashima, N.; Hamada, Y.; Matsumoto, A.; Kawakami, S.; Konishi, M.; Yamamoto, K.; Kumada, M. *Bull. Chem. Soc. Jpn.* **1980**, *53*, 1138.

(14) Zhao, Q.; Li, S.; Huang, K.; Wang, R.; Zhang, X. *Org. Lett.* **2013**, *15*, 4014.

(15) Selected reviews: (a) Beer, P. D.; Bayly, S. *Top. Curr. Chem.* **2005**, *255*, 125. (b) Bayly, S.; Beer, P. D.; Chen, G. Z. In *Ferrocenes: Ligands, Materials and Biomolecules*; Štěpnička, P., Ed.; Wiley: Chichester, U.K., 2008; Part II-Materials, Molecular Devices and Biomolecules, Chapter 8, pp 281−318.

(16) (a) Lamač, M.; Cvačka, J.; Štěpnička, P. *J. Organomet. Chem.* **2008**, *693*, 3430. (b) Lamač, M.; Císařová, I.; Štěpnička, P. *New J. Chem.* **2009**, *33*, 1549.

(17) Wuts, P. G. M.; Greene, T. W. *Protective Groups in Organic Chemistry*, 4th ed.; Wiley: Hoboken, NJ, 2007; Chapter 7, pp 696−926,

(18) (J. D. Riedel and A. de Häen AG, DE). Verfahren zur Darstellung von β-Aminoaethylharnstoff. German patent DE476533, 1925; SciFinder Scholar AN 1929:31367 (accessed January 20, 2013).

(19) El-Faham, A.; Albericio, F. *Chem. Rev.* **2011**, *111*, 6557.

(20) Štěpnička, P.; Císařová, I.; Podlaha, J.; Ludvík, J.; Nejezchleba, M. *J. Organomet. Chem.* **1999**, *582*, 319.

(21) Allen, F. H.; Kennard, O.; Watson, D. G.; Brammer, L.; Orpen, A. G.; Taylor, R. *J. Chem. Soc. Perkin Trans. 2* **1987**, S1 (Suppl.).

(22) Topologically, the hydrogen-bonded "strips" constituted by the independent molecules differ only in the presence of an additional, rather unfavorable (N12−H2N···O11 = 130°), and very likely conformation-enforced intramolecular N12···O11 interaction in molecule 1. An analogous contact in molecule 2, N22-H6N···O21, is only slightly longer (3.264(4) Å), but the H-bond angle is considerably more acute (113°), owing to conformational differences between the structurally independent molecules.

(23) (a) Etter, M. C. *Acc. Chem. Res.* **1990**, *23*, 120. (b) Custelcean, R. *Chem. Commun.* **2008**, 295.

(24) Pregosin, P. S.; Salzmann, R. *Coord. Chem. Rev.* **1996**, *155*, 35.

(25) Faller, J. W. In *Encyclopedia of Inorganic Chemistry*; King, R. B., Ed.; Wiley: New York, 1994; pp 3914−3933.

(26) Štěpnička, P.; Lamač, M.; Císařová, I. *Polyhedron* **2004**, *23*, 921.

(27) The relative abundance of the two contributing orientations differ from one compound to another, being 92:8 in **5b**, 60:40 in **5c**, 77:23 in **5f**, and 78:22 in **5g**.

(28) Štěpnička, P.; Císařová, I. *Collect. Czech. Chem. Commun.* **2006**, *71*, 279.

(29) Tauchman, J.; Císařová, I.; Štěpnička, P. *Dalton Trans.* **2011**, *40*, 11748.

(30) Appleton, T. G.; Clark, H. C.; Manzer, L. E. *Coord. Chem. Rev.* **1973**, *10*, 335.

(31) (a) Braunstein, P.; Matt, D.; Dusausoy, Y.; Fischer, J.; Mitschler, A.; Ricard, L. *J. Am. Chem. Soc.* **1981**, *103*, 5115. (b) Braunstein, P.; Matt, D.; Nobel, D.; Bouaoud, S. E.; Grandjean, D. *J. Organomet. Chem.* **1986**, *301*, 401 and also refs 32−34..

(32) Ma, J.-F.; Yamamoto, Y. *Inorg. Chim. Acta* **2000**, *299*, 164.

(33) Štěpnička, P.; Solařová, H.; Císařová, I. *J. Organomet. Chem.* **2011**, *696*, 3727.

(34) Tauchman, J.; Císařová, I.; Štěpnička, P. *Organometallics* **2009**, *28*, 3288.

(35) Ring puckering parameters are as follows: Q = 0.410(2) Å, φ = 41.8(3)°. The analysis can be taken only as informative because of varying interatomic distances. For a reference, see: Cremer, D.; Pople, J. A. *J. Am. Chem. Soc.* **1975**, *97*, 1354.

(36) Other organometallics such as BiR_3, InR_3 or organotins(IV) were shown to couple with boronic acids under Pd catalysis as well: (a) Barton, D. H. R.; Ozbalik, N.; Ramesh, M. *Tetrahedron* **1988**, *44*, 5661. (b) Rao, M. L. N.; Venkatesh, V.; Jadhav, D. N. *Tetrahedron Lett.* **2006**, *47*, 6975. (c) Rao, M. L. N; Jadhav, D. N.; Venkatesh, V. *Tetrahedron Lett.* **2009**, *50*, 4268. (d) Chen, J.-Y.; Chen, S.-C.; Tang, Y.-J.; Mou, C.-Y.; Tsai, F.-Y. *J. Mol. Catal. A: Chem.* **2009**, *307*, 88. (e) Pérez, I.; Pérez Sestelo, J.; Sarandeses, L. A. *J. Am. Chem. Soc.* **2001**, *123*, 4155. (f) Luong, M.; Domini, C. E.; Silbestri, G. F.; Chopa, A. B. *J. Organomet. Chem.* **2013**, *723*, 43 and references cited therein. For a review of earlier work, see: (g) Dieter, R. K. *Tetrahedron* **1999**, *55*, 4177.

(37) (a) Miyaura, N.; Suzuki, A. *Chem. Rev.* **1995**, *95*, 2457. (b) Wu, X.-F.; Neumann, H.; Beller, M. *Chem. Soc. Rev.* **2011**, *40*, 4986. (c) Ishiyama, T.; Kizaki, H.; Hayashi, T.; Suzuki, A.; Miyaura, N. *J. Org. Chem.* **1998**, *63*, 4726.

(38) Bykov, V. V.; Korolev, D. N.; Bumagin, N. A. *Russ. Chem. Bull.* **1997**, *46*, 1631.

(39) It must be noted that the Pd-catalyzed reaction of $Na[BPh_4]$ with acyl chlorides (RCOCl) to give ketones (PhCOR) was reported already in 1993: Cho, C. S.; Itotani, K.; Uemura, S. *J. Organomet. Chem.* **1993**, *443*, 253.

(40) See, for instance: Larock, R. C. *Comprehensive Organic Transformations*, 2nd ed.; Wiley-VCH: New York, 1999.

(41) (a) Kotha, S.; Lahiri, K.; Kashinath, D. *Tetrahedron* **2002**, *58*, 9633. (b) Blangetti, M.; Rosso, H.; Prandi, C.; Deagostino, A.; Venturello, P. *Molecules* **2013**, *18*, 1188.

(42) For examples, see: (a) Xin, B.; Zhang, Y.; Cheng, K. *J. Org. Chem.* **2006**, *71*, 5725 (reaction in water in the presence of poly(ethylene glycol) or 3-methylimidazolium hexafluorophosphate (or bmim[PF_6]). (b) Xin, B.; Zhang, Y.; Cheng, K. *Synthesis* **2007**, 1970 (reaction in water in the presence of sodium dodecyl sulfate).

(43) The reference ^{19}F NMR data were taken from: (a) Molander, G. A.; Cavalcanti, L. N.; Canturk, B.; Pan, P.-S.; Kennedy, L. E. *J. Org. Chem.* **2009**, *74*, 7364. (b) Crampton, R.; Woodward, S.; Fox, M. *Adv. Synth. Catal.* **2011**, *353*, 903.

(44) (a) Handy, S. T.; Bregman, H.; Lewis, J.; Zhang, X.; Zhang, Y. *Tetrahedron Lett.* **2003**, *44*, 427. (b) Navarro, O.; Kelly, R. A., III; Nolan, S. P. *J. Am. Chem. Soc.* **2003**, *125*, 16194. (c) Ghosez, L.; Franc, C.; Denonne, F.; Cuisinier, C.; Touillaux, R. *Can. J. Chem.* **2001**, *79*, 1827.

(45) This compound was chosen mainly because it can be easily converted to phenyl(4-chlorophenyl)methanol, a synthetic precursor of the widely applied antihistamine cetirizine (an active substance of Zyrtec etc.). See, for instance: Baltes, E.; De Lannoy, J.; Rodriguez, L. (UCB Pharmaceuticals, Inc.). 2-[4-(Diphenylmethyl)-1-piperazinyl]-acetic acids and their amides. US Patent 4525358, 1985.

(46) Miyaura, N. In *Metal-catalyzed cross-coupling reactions*, 2nd ed.; de Meijere, A., Diederich, F., Eds.; Wiley-VCH: Weinheim, Germany, 2004; Vol. *1*, Chapter 2, pp 41−123.
(47) Isosteric replacements are employed mostly in drug design and in biomedicinal research: (a) *Bioisosteres in Medicinal Chemistry*, Brown, N., Ed.; Wiley: Weinheim, Germany, 2012. (b) Patani, G. A.; LaVoie, E. J. *Chem. Rev.* **1996**, *96*, 3147.
(48) Moncol, J.; Coppens, P. *Private Communication to CCDC* (2004). Structure determined at 90 K.
(49) Chiari, G.; Taylor, H. C. R.; Fronczek, F. R.; Newkome, G. R. *Acta Crystallogr., Sect. B: Struct. Crystallogr. Cryst. Chem.* **1980**, *36*, 2488.
(50) Yu, A.; Shen, L.; Cui, X.; Peng, D.; Wu, Y. *Tetrahedron* **2012**, *68*, 2283.
(51) Zhang, L.; Wu, J.; Shi, L.; Xia, C.; Li, F. *Tetrahedron Lett.* **2011**, *52*, 3897.
(52) Štěpnička, P.; Solařová, H.; Císařová, I. *J. Organomet. Chem.* **2011**, *696*, 3727.
(53) Cope, A. C.; Friedrich, E. C. *J. Am. Chem. Soc.* **1968**, *90*, 909.
(54) Steffel, L. R.; Cashman, T. J.; Reutershan, M. H.; Linton, B. R. *J. Am. Chem. Soc.* **2007**, *129*, 12956.
(55) For a recently published, alternative synthesis, see: Mistry, S. N.; Baker, J. G.; Fischer, P. M.; Hill, S. J.; Gardiner, S. M.; Kellam, B. *J. Med. Chem.* **2013**, *56*, 3852.
(56) The deprotection procedure was adapted from: Lamač, M.; Tauchman, J.; Dietrich, S.; Císařová, I.; Lang, H.; Štěpnička, P. *Appl. Organomet. Chem.* **2010**, *24*, 326.
(57) For an alternative synthesis, see: Guddneppanavar, R.; Saluta, G.; Kucera, G. L.; Bierbach, U. *J. Med. Chem.* **2006**, *49*, 3204 and references cited therein.
(58) For alternative preparations, see: (a) Erhardt, P. W.; Woo, C. M.; Matier, W. L.; Gorczynski, R. J.; Anderson, W. G. *J. Med. Chem.* **1983**, *26*, 1109. (b) Kopka, K.; Wagner, S.; Riemann, B.; Law, M. P.; Puke, C.; Luthra, S. K.; Pike, V. W.; Wichter, T.; Schmitz, W.; Schober, O.; Schäfers, H. *Bioorg. Med. Chem.* **2003**, *11*, 3513. (c) Wiget, P. A.; Manzano, L. A.; Pruet, J. M.; Gao, G.; Saito, R.; Monzingo, A. F.; Jasheway, K. R.; Robertus, J. D.; Anslyn, E. V. *Bioorg. Med. Chem. Lett.* **2013**, *23*, 6799 and ref 56.
(59) Upon crystallization, **2a**·2HCl typically separates first.
(60) ^{1}H NMR (DMSO): δ 3.37 (br s, 4 H, CH_2), 8.50 (s, 6 H, NH_3). $^{13}C\{^{1}H\}$ NMR (DMSO): δ 36.45 (s, CH_2). The compound resulted upon addition of the stoichiometric amount of methanolic HCl to a solution of 1,2-diaminoethane in diethyl ether.
(61) Sheldrick, G. M. *Acta Crystallogr., Sect. A: Found. Crystallogr.* **2008**, *64*, 112.
(62) van der Sluis, P.; Spek, A. L. *Acta Crystallogr., Sect. A: Found. Crystallogr.* **1990**, *46*, 194.
(63) Spek, A. L. *J. Appl. Crystallogr.* **2003**, *36*, 7.